



**HAL**  
open science

## Absorption methods for the determination of mass transfer parameters of packing internals: A literature review

Laszlo Hegely, John Roesler, Pascal Alix, David Rouzineau, Michel Meyer

### ► To cite this version:

Laszlo Hegely, John Roesler, Pascal Alix, David Rouzineau, Michel Meyer. Absorption methods for the determination of mass transfer parameters of packing internals: A literature review. *AICHE Journal*, 2017, 63 (8), pp.3246-3275. 10.1002/aic.15737 . hal-01587673

**HAL Id: hal-01587673**

**<https://ifp.hal.science/hal-01587673>**

Submitted on 16 Oct 2018

**HAL** is a multi-disciplinary open access archive for the deposit and dissemination of scientific research documents, whether they are published or not. The documents may come from teaching and research institutions in France or abroad, or from public or private research centers.

L'archive ouverte pluridisciplinaire **HAL**, est destinée au dépôt et à la diffusion de documents scientifiques de niveau recherche, publiés ou non, émanant des établissements d'enseignement et de recherche français ou étrangers, des laboratoires publics ou privés.



## Open Archive Toulouse Archive Ouverte (OATAO)

OATAO is an open access repository that collects the work of some Toulouse researchers and makes it freely available over the web where possible.

This is an author's version published in: <http://oatao.univ-toulouse.fr/20424>

**Official URL:** <http://doi.org/10.1002/aic.15737>

### To cite this version:

Hegely, Laszlo and Roesler, John and Alix, Pascal and Rouzineau, David and Meyer, Michel Absorption methods for the determination of mass transfer parameters of packing internals: A literature review. (2017) *AIChE Journal*, 63 (8). 3246-3275. ISSN 0001-1541

Any correspondence concerning this service should be sent to the repository administrator:

[tech-oatao@listes-diff.inp-toulouse.fr](mailto:tech-oatao@listes-diff.inp-toulouse.fr)

# Absorption Methods for the Determination of Mass Transfer Parameters of Packing Internals: A Literature Review

Laszlo Hegely 

IFP Energies Nouvelles Lyon, Rond-point de l'échangeur de Solaize, Solaize 69630, France

INP Toulouse, Laboratoire de Génie Chimique, Toulouse 31432, France

John Roesler and Pascal Alix

IFP Energies Nouvelles Lyon, Rond-point de l'échangeur de Solaize, Solaize 69630, France

David Rouzineau and Michel Meyer

INP Toulouse, Laboratoire de Génie Chimique, Toulouse 31432, France

*Methods for the determination of mass-transfer coefficients and effective interfacial areas in packed absorption columns are reviewed. For each parameter, the methods are grouped into categories on the basis of their physical principle; the chemical systems used, experimental protocol, and the advantages and inconveniences are discussed. The treatment of end effects, the influence of packed bed height, and the recent efforts in standardization of measurement methods are also treated. The aim of the review is to give a broad overview of the methods used in literature in the last eight deca-des, some of which might be reconsidered in the light of modern measurement techniques and to evaluate them in relation to precision, practicality and hazardousness thereby to facilitate the search for reliable, precise, and convenient experimental practices.*

*Keywords: mass-transfer coefficient, interfacial area, absorption, desorption, packed column*

## Introduction

In counter-current separation processes, such as distillation, extraction, and gas absorption, the separation is based on the transfer of one or more components between the fluid phases in contact. To improve the efficiency of these processes by the increase of mass transfer between the phases, the contact between the phases is intensified by the application of phase contactor devices: trays (plates) or packings. The contact of the phases is stagewise in the case of trays, and continuous with packings. The use of packed columns is especially widespread in absorption owing to their advantages over tray columns. Packings offer lower pressure drop, higher capacity, and higher interfacial area. Random packings have been used since the beginning of the 20th century. They consist of discrete structural elements that are randomly dumped in a column to make the absorption section. Typical sizes range from 1 to 10 cm. Structured packings are made up of corrugated metal sheets or wire mesh that are placed vertically into the column as blocks of assembled layers. The corrugation sizes are typically between 0.5 and 2 cm with block sizes on the order of 25 cm. Structured packings are less commonly used in absorption.<sup>1</sup> They tend to be better suited for low pressure

applications as they offer particularly low pressure drop and increased capacity and efficiency, but at a higher cost.

For the design and analysis of separation columns reliable mass transfer parameters are needed, especially with the increased use of rate-based models for process simulations. Mass-transfer coefficients relate the mass transfer flux to the driving force which is the mass concentration potential difference inducing it. Depending on the choice of concentration difference, multiple mass-transfer coefficients can be defined. If the concentrations in the bulk phases are used, we speak of overall mass-transfer coefficients:

$$\varphi = K_G(y - y^*) = K_L(x^* - x) \quad (1)$$

where  $\varphi$  is the rate of absorption per unit surface ( $\text{mol}/[\text{m}^2 \text{ s}]$ ),  $K_G$  is the gas-side,  $K_L$  is the liquid-side overall mass-transfer coefficient ( $\text{mol}/[\text{m}^2 \text{ s}]$ ),  $y$  is the mole fraction of the solute in the gas phase, and  $x$  is the mole fraction in the liquid phase. The superscript \* denotes an equilibrium concentration: for example,  $y^*$  is the gas phase solute concentration at equilibrium with the liquid bulk solute concentration  $x$ . Note that  $K_G$  and  $K_L$  have the same physical meaning; they are just written from the perspective of the gas or of the liquid phases.

The mass-transfer coefficients of the individual phases ( $k_G$  for gas and  $k_L$  for liquid) characterize the mass transfer conductance of their respective phases and therefore have different physical meanings. In this case, the driving force is written as the difference between the bulk and interfacial concentration:

<sup>1</sup>Correspondence concerning this article should be addressed to L. Hegely at this current address: Budapest University of Technology and Economics, H-1111, Budapest, Muegyetem rkp. 3-9; e-mail: hegelyl@hotmail.com.

$$\varphi = k_G(y - y_i) = k_L(x_i - x) \quad (2)$$

where index  $i$  refers to the interface. The overall resistance to mass transfer between the two phases is the sum of the resistances of the individual phases. The overall gas-side mass-transfer coefficient  $K_G$  is then expressed as:

$$\frac{1}{K_G} = \frac{1}{k_G} + \frac{m}{k_L} \quad (3)$$

where  $m$  gives the equilibrium relation between gas- and liquid-side concentrations:

$$y = mx \quad (4)$$

If a chemical reaction is consuming the solute in the liquid phase then the absorption flux will be accelerated and the effective liquid-side mass-transfer coefficient is then expressed as  $k_{L,R}$ , the value of which is greater than  $k_L$ .

The individual determination of each film coefficient would require measurements of interfacial and bulk concentrations of the solute. However, current experimental techniques are not capable of interfacial measurements. The individual film coefficients can thus only be determined under conditions where the resistivity of one of the phases is neglected. Various reactive absorption methods have been used to approach such conditions but the only case when there is absolutely no resistivity in one of the phases is when this phase is purely the solute because there is then no concentration gradient. In every other situation, neglecting the resistivity is an approximation, the validity of which has to be verified.

The total absorption rate per unit volume of packing depends directly on the exchange area available that is characterized by the effective interfacial area mass transfer parameter  $a_e$  ( $\text{m}^2/\text{m}^3$ ):

$$\Phi = a_e \varphi = k_G a_e (y - y_i) = k_L a_e (x_i - x) \quad (5)$$

Experimental measurements of concentrations changes in one of the phases yields  $\Phi$  from which  $k_G a_e$  and  $k_L a_e$  can then be derived. The values of  $k_G$  and  $k_L$  are then obtained by dividing by  $a_e$  obtained from separate measurements. Errors in  $a_e$  will propagate into the mass-transfer coefficients. To avoid excessive uncertainties, it is therefore best to use mass transfer parameters obtained all in the same facility. In particular, when sizing a column with  $k_G$  or  $k_L$  correlations, the latter should be used only with the effective area correlation from which they were derived in order to be coherent with experimentally measured absorption rates.

The mass transfer performance of a packed column can be expressed either on the basis of transfer units or theoretical plates. The change in composition of one of the phases is given by:

$$\int_{y_{\text{out}}}^{y_{\text{in}}} \frac{1}{y - y^*} dy = \frac{HK_G a_e}{G} \quad (6)$$

where  $G$ , the column gas molar flow rate per sectional area ( $\text{mol}/[\text{m}^2 \cdot \text{s}]$ ), is assumed constant and  $a_e$  is the effective interfacial area ( $\text{m}^2/\text{m}^3$ ). If the equilibrium concentration  $y^*$  is constant between inlet and outlet then this equation describes an exponential decay law towards equilibrium. One transfer unit is then defined to represent a fractional progress of 63% or  $1 - e^{-1}$  toward this equilibrium condition in the phase considered. This happens when the integrated term is equal to unity, which leads to the definition of the height of one transfer unit:

$$\text{HTU}_{\text{OG}} = \frac{G}{K_G a_e} \quad (7)$$

The number of transfer units of a column where the integral is not unity is then defined as:

$$\text{NTU}_{\text{OG}} = \frac{H}{\text{HTU}_{\text{OG}}} = \frac{HK_G a_e}{G} \quad (8)$$

Analogous equations can be derived for the liquid phase, as well:

$$\int_{x_{\text{out}}}^{x_{\text{in}}} \frac{1}{y - y^*} dx = \frac{HK_L a_e}{L} \quad (9)$$

$$\text{HTU}_{\text{OL}} = \frac{L}{K_L a_e} \quad (10)$$

$$\text{NTU}_{\text{OL}} = \frac{H}{\text{HTU}_{\text{OL}}} = \frac{HK_L a_e}{L} \quad (11)$$

where  $L$  is the molar flux of the liquid ( $\text{mol}/[\text{m}^2 \cdot \text{s}]$ ).  $\text{NTU}_{\text{OG}}$  and  $\text{NTU}_{\text{OL}}$  have different numerical values, but both can be applied, as long as the appropriate HTU value is used. Depending on the composition difference, and thus on the mass-transfer coefficient used, NTU and HTU can be of overall nature (gas- or liquid-side) or defined for one of the phases only. They are determined experimentally by measuring concentration changes in one of the phases between the inlet and outlet of the column. They characterize volumetric mass-transfer coefficients  $k_G a_e$  or  $k_L a_e$ .

While transfer units are preferred in absorption, the concept of height equivalent to a theoretical plate (HETP) is applied widely in distillation design. The height of packed bed is then expressed as the product of the number of theoretical plates and the HETP. Both HETP and HTU measure the performance of the packing, although HTU-NTU method is physically more fundamental.

Ever since the introduction of the two-film theory of interfacial mass transfer in the 1920s, a vast number of studies has been performed for the determination of the mass transfer parameters  $k_G a_e$ ,  $k_L a_e$  and  $a_e$  of different random and structured packings, using a variety of methods. Based on measurement results, a large number of empirical and semi-empirical (based on theoretical considerations) correlations have been proposed for these mass transfer parameters expressed in terms of operating conditions, packing geometry, and physical properties of the gas and liquid phases. An extensive review of these correlations has been given by Wang et al.<sup>2</sup> Considering just the last 20 years, Figure 1 illustrates that even recent correlations lead to considerably different calculated mass transfer parameter values. These disparities reflect those of experimental results obtained in the various apparatus, and illustrate the need for a cautious evaluation of experimental methods. Part of the differences may result from using the correlations beyond their range of validity whether they are hydraulic or fluid physical property parameters. The latter situation can easily arise despite the inclusion of viscosity, density, or surface tension terms in the correlations, simply because the underlying experiments have usually been performed within only a small range of values, if any, of such properties. Extrapolation to other packings can be more successful (especially for structured packings) when terms related to the packing geometry are taken into account.

The above discussion shows the need for improving the precision and accuracy of experimental methods in order to

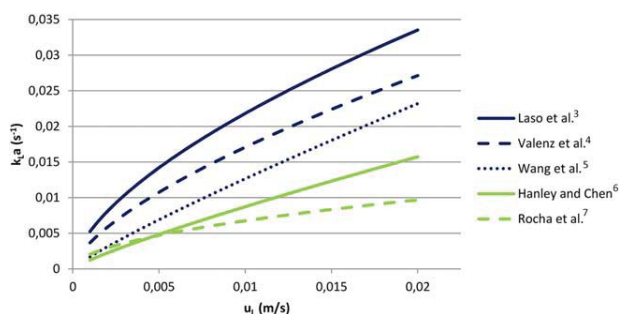


**Figure 1. An example for the deviation of correlations: predicted  $k_L a$  values for Mellapak 250.Y (based on Wang et al.<sup>5</sup>).**

The  $k_L a$  values are adjusted to the toluene-water system of Wang et al.<sup>5</sup> by assuming square-root dependency to liquid side diffusivity of the solute. [Color figure can be viewed at [wileyonlinelibrary.com](http://wileyonlinelibrary.com)]

derive reliable and coherent sets of data. Errors can originate from a number of sources such as hydrodynamic uncertainties, by neglecting or underestimating end-effects, and phase maldistributions, chemical uncertainties, leading to ill assessment of the absorption regime, or yet underestimating the contribution of one of the phases to the mass transfer resistance, etc.<sup>8</sup> In light of these difficulties, several authors insisted in recent years on the standardization of the methods.<sup>8–10</sup>

The aim of the present work is to give a comprehensive overview of the experimental methods that have been used to determine the mass transfer parameters  $k_G$ ,  $k_L$ , and  $a_e$ , from the earliest experiments in the 1920s to the most recent investigations. This work brings up to date previous more specific reviews on the determination of  $a_e$ ,<sup>11</sup> or on the different chemical methods for the determination of all three parameters<sup>12,13</sup> along with a review of broader scope<sup>14</sup> and complements recent articles<sup>8,9</sup> that cover only partial lists of the possible methods. We have chosen to make a broad review in order to assess the possibility of reconsidering older methods that may be worthy in light of modern analytical techniques. For every method, references are given along with the packing type and chemical system used. Correlations established based on the experiments are not included, as they are not likely to be directly comparable to each other due to different gas and liquid load and packings applied. Some of these correlations can be found in the review of Wang et al.<sup>2</sup> It would be also interesting to collect experimental data obtained under the same conditions by different authors and compare them also with predicted data, however, this is outside the scope of the present work, and could be the subject of a future paper. We must also note that although this article focuses on packings, the methods reviewed could equally be applied to the determination of mass transfer parameters of other types of column internals, such as trays or spray nozzles.

Methods for each of the mass transfer parameters  $k_G$ ,  $k_L$ , and  $a_e$  are presented and discussed separately, categorizing the measurement techniques by physical or chemical principle. Different procedures to estimate end-effects, packed bed height effects on the mass transfer parameters are also reviewed and discussed as they are an integral part of the source of data disparity among authors. Last, we review the literature proposals for standardization of the measurement methods.

## Determination of the Effective Interfacial Area

Knowledge of the effective interfacial area for mass transfer is crucial, especially since errors in its evaluation will propagate into the determination of  $k_G$  and  $k_L$  that are calculated by dividing the volumetric mass-transfer coefficients by the interfacial area, for example:

$$k_G = \frac{k_G a_e}{a_e} \quad (12)$$

Moreover, according to Ahmadi<sup>15</sup> and Maćkowiak and Maćkowiak,<sup>16</sup> the results of rate-based models for column and process design are particularly sensitive to the value of  $a_e$ .

In the literature dealing with column packings, different methods have been developed to determine the area, however, they do not always measure the same type of area. The methods can be classified into the following groups based on the physical or chemical measurement principle:

- chemical absorption,
- vaporization of a pure liquid,
- physical absorption,
- tomography,
- colorimetry,
- sublimation of the packing.

The value and significance of the determined area varies according to the type of method used. Some measure the interfacial area, others a wetted area and others yet an effective area all of which can have different values. It is very important to clearly state what type of area is measured for its appropriate use in subsequent calculations. For example, a correlation for “ $a$ ” obtained by evaporation would not be appropriate for use in a physical absorption process calculation due to saturation of stagnant zones that would reduce the effective area for mass transfer of a solute but not for evaporation. This is one of the reasons why film mass-transfer coefficient correlations should be used with the corresponding area correlation from which they were derived, and not mixed between different authors.

In the following sections, we first review the definitions and significance of the various types of areas encountered in packings. Then the different types of methods will be discussed, highlighting also the nature of the interfacial area measured.

### Specific areas defined in packings

In the literature dealing with column packings, several types of specific areas are defined. To illustrate these areas, Figure 2 schematizes a liquid flow around a single packing element such as a Raschig ring.

The geometric area of the packing elements per unit volume of column,  $a_g$ , can be calculated from the dimensions of the packing. It is a fixed quantity for structured packings, but in the case of random packings, it depends on the filling density, or the number of packing elements per  $m^3$ .

The wetted area  $a_w$  is defined as the portion of the geometric area covered with liquid. By definition, it cannot be larger than the latter. The value of the wetted area is influenced by the gas and liquid flow distribution patterns and the wettability of the packing. The latter is determined by the surface tension of the liquid and the packing material. Plastic packings have lower wettability than metal and ceramic ones. Porosity and surface roughness increase wettability.

The interfacial area,  $a_i$ , is defined as the total contact surface between the gas and liquid phases. This area is not clearly distinguished from  $a_w$  in the literature; the majority of the articles

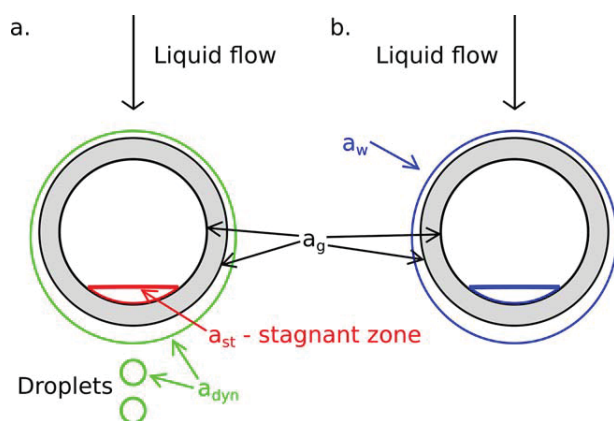


**Figure 2. Different surface areas identified schematically for liquid flowing around a single Raschig ring: (a) static and dynamic areas, (b) wetted area.**

[Color figure can be viewed at [wileyonlinelibrary.com](http://wileyonlinelibrary.com)]

claiming to determine  $a_w$  implicitly assume that liquid is only present on the surface of packings. However, liquid between packing elements in the form of droplets and rivulets, and liquid on the column wall contribute to mass transfer, meaning that  $a_i$  is always higher than  $a_w$ . The ratio between the two areas is greater for random than for structured packings.<sup>17</sup> Puranik and Vogelpohl<sup>18</sup> discriminate between a static ( $a_{st}$ ) and a dynamic ( $a_{dyn}$ ) part of the interfacial area (although they considered it to be equal to  $a_w$ ), assuming that they are the interfacial area belonging to static and dynamic liquid hold-up, respectively:

$$a_i = a_{st} + a_{dyn} \quad (13)$$

The static part of interfacial area is not renewed, thus it is affected by saturation or depletion of the solute or of chemicals, and after some time no longer participates in the mass flux. Its ratio to the total interfacial area is likely to be higher for early random packings such as Raschig rings, and lower for structured and modern random packings, which have more open forms, as one of the main goals of the development of new packings is the elimination of stagnant liquid pools. The dynamic part of the wetted area is continuously renewed by the liquid flow, and thus remains active for mass transfer of the solute.

Last and most important is the effective interfacial area,  $a_e$ , which is the part of the interfacial area, where mass transfer actually takes place. Its value can be very different from the geometric and/or wetted areas. It is always lower than the interfacial area, since a fraction of  $a_i$  may be inactive due to stagnation and local saturation or depletion of a species in the liquid bulk. In addition, liquid can flow along the column wall as well as between packing elements (droplets, rivulets) and thereby increase the effective area relative to the geometric area, more so with random packings than with structured ones.<sup>17</sup> Kolev et al.<sup>19</sup> have reported instances where  $a_e$  is twice the value of  $a_g$ .

The magnitude of the effective interfacial area depends on the nature of the mass transfer process taking place in the column. With evaporation of a pure liquid, the entire interfacial area is active since there is no concentration change in the liquid phase. With physical absorption,  $a_e$  is lower than  $a_i$  and

equal to  $a_{dyn}$ . The stagnant liquid parts, that is, the zones without a sufficiently high liquid flow rate and/or turbulence to ensure renewal of the phase, become saturated with the solute, so they become inactive. In the case of desorption, the same situation occurs due to depletion of the solute. Shulman<sup>20,21</sup> related the ratio of  $a_e$  and  $a_{dyn}$  to that of total and dynamic liquid hold-up. With chemical absorption, the reaction rate and the change of solvent capacity have important effects. This is described by Joosten and Danckwerts<sup>22</sup> with a parameter  $\gamma_{JD}$  defined as:

$$\gamma_{JD} = \frac{C}{E} \quad (14)$$

where  $C$  is the factor by which the reaction increases the absorption capacity per liquid unit volume,  $E$  is the enhancement factor, that is, the ratio of the absorption rates with and without reaction. In the case of a slower reaction with high absorbent capacity (e.g., buffer solutions),  $\gamma_{JD} \gg 1$ , the liquid does not become saturated and the entire liquid surface will be active for mass transfer. However, if  $\gamma_{JD} = 1$ , such as with an instantaneous reaction, then although a greater quantity of the solute can be absorbed in the liquid than without reaction, the rate of absorption increases proportionally to the capacity, such that the time to saturate the stagnant liquid zones is unchanged. This means that saturation will reduce the effective area, which will be equal to the one in the case physical absorption.

Puranik and Vogelpohl<sup>18</sup> proposed correlations for  $a_{st}$  and  $a_e$  of random packings based on available literature data. Their correlations apply to various mass transfer situations, and can be used to illustrate the differences of  $a_e$  under different situations. Figure 3 shows the values calculated as a function of liquid load within the range of validity for a packing with  $a_g = 300 \text{ m}^2/\text{m}^3$ , using water as liquid. The static area in the correlation depends only on the properties of the liquid and  $a_g$ , giving a constant  $a_e/a_g$  in our calculation. The effective interfacial area is shown for different absorption situations with different values of the Hatta number ( $Ha$ ) with the latter varying only from an increase in the liquid phase reagent concentration. In this case,  $C$  increases faster with the reagent concentration than  $E$ . Physical absorption corresponds to the situation where  $Ha$  is zero, and  $a_e = a_{dyn}$ . The case of  $Ha = 1$  corresponds to an intermediate reaction speed. As  $Ha$  increases, an increasing part of  $a_{st}$  becomes effective for the mass transfer, and thus the effective area increases:  $a_e = \eta(Ha) \cdot a_{st} + a_{dyn}$ . The case with  $Ha = \infty$  corresponds to an infinitely fast reaction, the limiting case where the entire interfacial area is effective that is  $a_e = a_{st} + a_{dyn}$ . Thus the difference between the solid grey line ( $Ha = 0$ ) and the dashed black line ( $Ha = \infty$ ) is simply  $a_{st}$ . According to these correlations,  $a_{st}$  is significant, and of the same order of magnitude as  $a_e$  and actually higher than  $a_e$  at low liquid flow rates and  $Ha$ . These results illustrate the importance of assessing the type of area that is measured or applicable for a given measurement method.

In summary, several types of area can be defined and measured in packed columns. The values of these area may be significantly different, so it is important to be aware of the type of area that is obtained and to be cautious to use the appropriate one for a given absorption situation. For example,  $a_i$  can be used to determine  $k_G$  from  $k_G a$  measured by vaporization, but  $a_{dyn}$  should be used for physical absorption and  $a_e$  for chemical absorption.

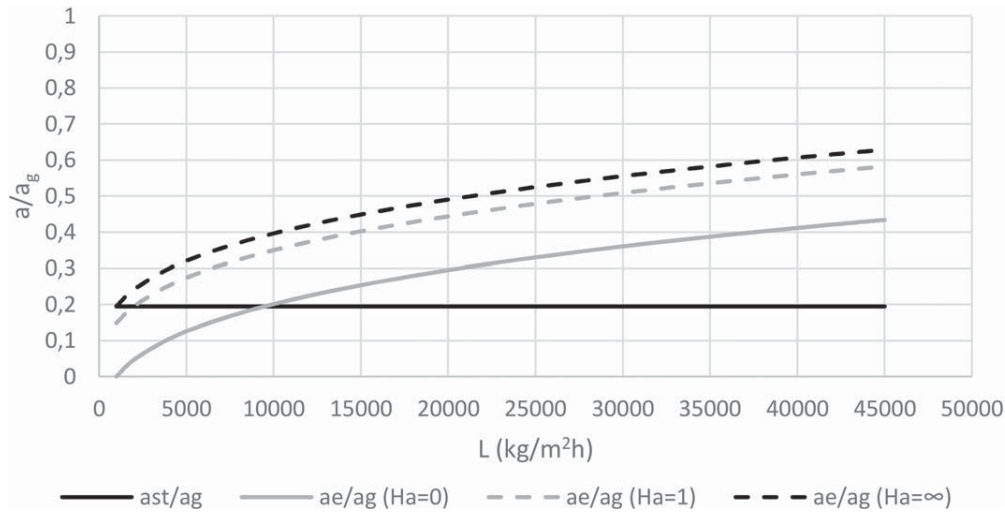


**Figure 3. Static and effective interfacial area calculated by the correlations of Puranik and Vogelpohl<sup>18</sup> for a random packing with  $a_g = 300 \text{ m}^2/\text{m}^3$ , with water as liquid phase.**

### Chemical absorption

The most popular method for determining  $a_e$  is chemical absorption with a reaction system in either the fast or intermediate reaction regimes. Overviews of this group of methods are given by Sharma and Danckwerts<sup>12</sup> and Laurent et al.<sup>13</sup> as applied to simple systems with analytical solutions. Last and Stichlmair<sup>23</sup> propose a method using fast second-order reactions, but to our knowledge, it has not yet been applied experimentally. In some of the more recent works,<sup>24,25</sup> complete column models have been developed, which are used to determine the interfacial area by using the latter as regression parameter to match measured mass transfer fluxes. In this section, we will describe these various methods and the chemical systems with which they have been applied.

Prior to discussing the methods, it is important to define two dimensionless numbers: the enhancement factor ( $E$ ) and the Hatta number ( $Ha$ ). The enhancement factor expresses the extent with which the chemical reaction increases the rate of absorption compared to physical absorption:

$$E = \frac{k_{L,R}}{k_L} \quad (15)$$

where  $k_{L,R}$  is the mass-transfer coefficient with chemical reaction. The Hatta number is the ratio of the rate of reaction to the rate of diffusion in the liquid film. As  $Ha$  increases,  $E$  converges to the enhancement factor of infinitely fast reaction  $E_{\text{inf}}$ . In this hypothetical case, the reaction takes place exclusively on the interface. For a detailed treatment of absorption in the presence of reactions, the reader is referred to the book of Danckwerts.<sup>26</sup> A classification of reaction regimes and corresponding expressions relating  $E$  and  $Ha$  can also be found in Last and Stichlmair.<sup>23</sup>

**Fast Reactions.** Literature studies using fast chemical absorption systems for the determination of  $a_e$  are listed in Table 1. They apply the methodology and chemical systems that are described hereafter.

**Methodology.** In order to determine  $a_e$  by chemical reaction, we need to know the reaction kinetics and the system must satisfy several constraints:

- negligible gas side resistance,

- $Ha \ll E_{\text{inf}}$ ,<sup>28,58</sup>
- $Ha > 3$ .<sup>12,29</sup>

The first constraint ensures that the concentration of solute at the interface is the same as in the bulk gas. The second constraint ensures that the reaction system is of pseudo- $m$ th order relative to the solute, which simplifies the analysis, as the concentration of the liquid phase reagent is constant in the film, and the third sensitizes the measured rate of absorption to  $a_e$  by effectively removing any dependence to (physical) liquid-side mass-transfer coefficient.

More precise forms of the second constraint are given by Henriques de Brito et al.<sup>41</sup> as:

$$Ha < \frac{1}{2} E_{\text{inf}} \quad (16)$$

and by Tsai et al.<sup>17</sup> as:

$$Ha < \frac{1}{5} E_{\text{inf}} \quad (17)$$

Other forms of the third condition can be found in the literature, such as  $Ha > 5$ ,<sup>13</sup>  $Ha > 2$ ,<sup>44</sup>  $E > 5$ ,<sup>27</sup> or  $E > 3$ .<sup>19</sup> The reactions fulfilling these constraints are sometimes called moderately fast,<sup>12</sup> to emphasize that they are not very fast or instantaneous reactions.

To illustrate the method of chemical absorption with fast reaction, consider the following irreversible reaction:



where  $A$  is the absorbed component,  $B$  is the reagent in the liquid phase,  $\nu$  is the stoichiometric coefficient, and the local rate of reaction is  $k[A]^m[B]^n$  with  $k$  the rate constant. For the above reaction,  $E_{\text{inf}}$  can be expressed as<sup>28,58</sup>:

$$E_{\text{inf}} = 1 + \frac{D_B B^0}{D_A \nu A^*} \quad (19)$$

where  $B^0$  is the bulk concentration of  $B$ ,  $A^*$  is the concentration of  $A$  at the surface of the liquid phase, and  $D_A$  and  $D_B$  ( $\text{m}^2/\text{s}$ ) are the diffusivities of  $A$  and  $B$  in the liquid phase.

The first constraint, negligible gas phase resistance, ensures that  $A^*$  is the solubility of  $A$  in the liquid phase without reaction as determined by the bulk gas phase concentration of  $A$ .

**Table 1. Investigations Using Chemical Absorption with a Fast Reaction to Determine  $a_c$**

Source	Packing	Gas	Liquid	Order of Reaction
Yoshida and Miura <sup>27</sup>	Raschig rings	CO <sub>2</sub> in air	NaOH (aq) KOH (aq)	Pseudo-first
Widwans and Sharma <sup>28</sup>	Raschig rings	CO <sub>2</sub> in air	NaOH (aq) MEA (aq)	Pseudo-first
Jhaveri and Sharma <sup>29</sup>	Raschig rings	Isobutylene O <sub>2</sub> of air	H <sub>2</sub> SO <sub>4</sub> CuCl + CuCl <sub>2</sub> + HCl (aq) dithionite + NaOH (aq)	Pseudo-first or pseudo-zero
Danckwerts and Rizvi <sup>30</sup>	Raschig rings, Pall rings, Intalox saddles	O <sub>2</sub> of air	Na <sub>2</sub> SO <sub>3</sub> + CoSO <sub>4</sub> (aq)	Second
Onda et al. <sup>31</sup>	Raschig rings	Pure O <sub>2</sub> , O <sub>2</sub> in air, O <sub>2</sub> of air	Na <sub>2</sub> SO <sub>3</sub> + CoSO <sub>4</sub> (aq)	Pseudo-first and pseudo-second
Sahay and Sharma <sup>32</sup>	Raschig rings, Pall rings, Intalox saddles	O <sub>2</sub> of air	dithionite (aq)	Pseudo-first and pseudo-second
Linek et al. <sup>33,34</sup>	Raschig rings, Pall rings	CO <sub>2</sub> in air	NaOH (aq) DEA (aq)	Pseudo-first
Alper <sup>35</sup>	Raschig rings, Pall rings	Pure O <sub>2</sub>	Na <sub>2</sub> SO <sub>3</sub> + CoSO <sub>4</sub> (aq)	Pseudo-second
Merchuk <sup>36</sup>	Fenske helices, porous ceramic cylinders	O <sub>2</sub> of air	Na <sub>2</sub> SO <sub>3</sub> + CoSO <sub>4</sub> (aq)	Pseudo-second
Rizzuti et al. <sup>37</sup>	Raschig rings, flat rings, spi- rals, saddles	CO <sub>2</sub> in air	NaOH (aq)	Pseudo-first
Neelakantan and Gehlawat <sup>38</sup>	Rings	O <sub>3</sub> in air	Phenol + base (aq)	Pseudo-zero
Linek et al. <sup>39</sup>	Raschig rings	Pure O <sub>2</sub>	(NH <sub>3</sub> ) <sub>2</sub> SO <sub>3</sub> (aq)	Pseudo-first
Weiland et al. <sup>40</sup>	Pall rings	CO <sub>2</sub> in air	NaOH (aq)	Pseudo-first
Henriques de Brito et al. <sup>41</sup>	Goodloe, Montz A2	CO <sub>2</sub> in air	NaOH (aq)	Pseudo-first
Benadda et al. <sup>42</sup>	Raschig rings, Mellapak 125.Y, 250.Y, 500.Y	CO <sub>2</sub> in air	NaOH (aq)	Pseudo-first
Weimer and Schaber <sup>43</sup>	Raschig rings	O <sub>2</sub> (21%)	Na <sub>2</sub> SO <sub>3</sub> + CoSO <sub>4</sub> (aq) CuCl (aq)	Pseudo-first
Nakajima et al. <sup>44</sup>	Mellapak 250.Y, Hiflow	CO <sub>2</sub> of air	NaOH (aq) KOH (aq)	Pseudo-first
Duss et al. <sup>45,46</sup> ; Duss and Menon <sup>47</sup>	Raschig rings, Pall rings	CO <sub>2</sub> in N <sub>2</sub>	NaOH + sugar (aq)	Pseudo-first
Kolev et al. <sup>19</sup> ; Nakov et al. <sup>48</sup>	Nutter rings	CO <sub>2</sub> of air	NaOH (aq)	Pseudo-first
Hoffmann et al. <sup>8</sup>	Raschig Super-Ring	CO <sub>2</sub> in air	NaOH (aq)	Pseudo-first
Green <sup>49</sup>	Pall rings	CO <sub>2</sub> in air	NaOH (aq)	Pseudo-first
Tsai et al. <sup>17,50,51</sup>	Mellapak 250.Y	CO <sub>2</sub> of air	NaOH (aq)	Pseudo-first
Alix and Raynal <sup>52</sup> ; Alix et al. <sup>53</sup>	Mellapak 250.X, 250.Y, 250.YS, 500.Y, 2Y, Mella- pak Plus 252.Y Flexipac 1Y, Prototype 500	CO <sub>2</sub> in air, or of air	NaOH (aq)	Pseudo-first
Aferka et al. <sup>54</sup>	IMTP50, 4D	CO <sub>2</sub> of air	NaOH (aq)	Pseudo-first
Valenz et al. <sup>4</sup>	Mellapak 752.Y	CO <sub>2</sub> of air	NaOH (aq)	Pseudo-first
Wang et al. <sup>55,56</sup>	Mellapak 250.Y, 350.Y, 452.Y, 500.Y	O <sub>2</sub> of air, or in pure form	Na <sub>2</sub> SO <sub>3</sub> + CoSO <sub>4</sub> (aq)	Pseudo-second
Rejl et al. <sup>57</sup>	Mellapak 2X, 250.X, 250.Y, Flexipac, Raschig Super- Pak, Raschig Super-Ring, Pall rings, GT-Pak 350Y, 350Z	CO <sub>2</sub> in air	NaOH (aq)	Pseudo-first
Kunze et al. <sup>10</sup>	Super-Pak 250.Y	CO <sub>2</sub> in air	NaOH (aq)	Pseudo-first
	Pall rings, Mellapak 250.Y	CO <sub>2</sub> of air	NaOH (aq)	Pseudo-first

The second constraint ensures that the reaction is of pseudo- $m$ th order by keeping the concentration of  $B$  constant through the liquid film (equal to  $B^0$ ) which rules out very fast reactions and also means that a great excess of  $B$  is preferred in the experiments. Component  $A$  reacts within a very short distance of the interface, such that its concentration is zero in the bulk of the liquid phase.<sup>29</sup> Then the rate of absorption per unit volume ( $\Phi$ , mol/[m<sup>3</sup>·s]) can then be written as:

$$\Phi = Ek_L a_c A^* \quad (20)$$

and the Hatta number is then given as<sup>12</sup>:

$$\text{Ha} = \frac{\sqrt{\frac{2}{m+1} D_A k (A^*)^{m-1} (B^0)^n}}{k_L} \quad (21)$$

The third constraint ensures that the reaction is still fast enough so that the rate of physical absorption is negligible

compared to reaction rate, eliminating thereby the dependency of  $E$  on  $k_L$ . In this reaction regime, where the second and third constraints are valid, the following relation is true for the double-film model:

$$E = \frac{\text{Ha}}{\tanh \text{Ha}} \quad (22)$$

and consequently  $E \approx \text{Ha}$ . Sometimes the condition is even formulated as the assumption of  $E = \text{Ha}$ .<sup>8,53</sup> By substitution into Eq. 20,  $k_L$  is eliminated and  $\Phi$  becomes directly proportional to  $a_c$ :

$$\Phi = a_c A^* \sqrt{\frac{2}{m+1} D_A k (A^*)^{m-1} (B^0)^n} = a_c A^* \sqrt{D_A k_R} \quad (23)$$

with

**Table 2. Main Characteristics of the Methods Using the Danckwerts' Plot to Determine  $a_e$**

Source	Packing	Gas	Liquid
Danckwerts and Gillham <sup>60</sup>	Raschig rings	Pure CO <sub>2</sub> (saturated with water vapor)	K <sub>2</sub> CO <sub>3</sub> + KHCO <sub>3</sub> + NaOCl (aq) NaOH + Na <sub>2</sub> SO <sub>4</sub> (aq) Na <sub>2</sub> SO <sub>4</sub> (aq)
Jhaveri and Sharma <sup>29</sup>	Raschig rings	O <sub>2</sub> of the air	CuCl + HCl (aq)
Joosten and Danckwerts <sup>22</sup>	Raschig rings, Intalox saddles	Pure CO <sub>2</sub>	KHCO <sub>3</sub> + K <sub>2</sub> CO <sub>3</sub> + KAsO <sub>2</sub> (aq)
Rizzuti et al. <sup>37,61</sup>	Raschig rings	Pure CO <sub>2</sub>	K <sub>2</sub> CO <sub>3</sub> + KHCO <sub>3</sub> + KAsO <sub>2</sub> + sugar (aq)
Rizzuti and Brucato <sup>62</sup>			
Alper <sup>35</sup>	Fenske helices, porous ceramic cylinders	Pure CO <sub>2</sub>	K <sub>2</sub> CO <sub>3</sub> + KHCO <sub>3</sub> + KAsO <sub>2</sub> (aq)
Benadda et al. <sup>42</sup>	Raschig rings	CO <sub>2</sub> (10%)	Na <sub>2</sub> CO <sub>3</sub> + NaHCO <sub>3</sub> + NaOCl (aq)
Roesler and Raynal <sup>63</sup>	SMV8X	CO <sub>2</sub> (10%)	Na <sub>2</sub> CO <sub>3</sub> + NaHCO <sub>3</sub> + NaOCl (aq)

$$k_R = \frac{2}{m+1} k(A^*)^{m-1} (B^0)^n \quad (24)$$

representing the reaction term. So then, the effective area is given as:

$$a_e = \frac{\Phi}{A^* \sqrt{D_A k_R}} \quad (25)$$

To determine  $a_e$  experimentally, the rate of absorption per unit volume  $\Phi$  is obtained by measuring the solute concentration changes under various operating conditions, while the other parameters are obtained from different sources. If the kinetics parameters are known,  $k_R$  can be calculated, otherwise, it can be determined in model apparatus, such as wetted-wall columns, non-aerated reactors,<sup>33,34</sup> stirred cells, or jet apparatus.<sup>29</sup> In selecting the chemical system and reactant composition, caution must be exercised to verify that  $k_R$  is not too high so as to induce gas-side resistance. However, if this is the case, methods have been described to take into account this additional factor<sup>52</sup> as described in the section "Determination of the Gas-Side Mass-Transfer Coefficient—Chemical absorption."

**Chemical Systems.** For fast pseudo- $m$ th order reactions, the most popular system used is the chemical absorption of CO<sub>2</sub> into a liquid solution of NaOH (Table 1). This system has two main advantages: the kinetics and physical parameters are well established<sup>59</sup> and the components are readily available. The absorption of the CO<sub>2</sub> naturally in air is a particularly practical solution. As shown in Table 1, in recent years researchers have used this system exclusively.

Other chemical systems applied in the past have included the absorption of CO<sub>2</sub> into other reagents (KOH, amines), or of O<sub>2</sub> into solutions of dithionite, sodium sulfite with CoSO<sub>4</sub> as catalyst, and CuCl. In some of these systems, the reaction order may change with reactant concentration; this is the case with O<sub>2</sub> and sulfites,<sup>31</sup> with which the order can range from 1 to 2. Deckwer<sup>58</sup> and Henriques de Brito et al.<sup>41</sup> discourage the use of this last system, because of kinetic rate uncertainties. Alper,<sup>35</sup> however minimized uncertainties and achieved sufficient accuracy with this system by performing kinetic measurements in a stirred cell with liquid samples for each of his absorption runs. Sharma and Danckwerts<sup>12</sup> recommend the use of the absorption of CO<sub>2</sub> into NaOH, KOH, or amines, although they warn about gas-side resistance becoming non-negligible. They state that the use of NaOH or KOH is very convenient. For laboratory use, they also propose the absorption of O<sub>2</sub> into solutions of CuCl and dithionite. The system O<sub>2</sub>–CuCl is, however, corrosive.

The constraints on the reaction speed need to be assessed over the whole column even for well-known absorption

systems. For example, Alix and Raynal<sup>52</sup> found that the constraints are not fully met for the absorption of CO<sub>2</sub> diluted with air into 1 N NaOH solution due to appreciable gas-side resistance. To avoid this problem, they suggest using a more dilute system with only a 0.1 N NaOH solution to reduce gas-side resistance and only the CO<sub>2</sub> of air to avoid excessively loading the liquid solution.

The use of pure solute in the gas phase eliminates the gas-side mass transfer resistance. Most often, however, the solute gases are diluted mixed with a carrier gas, typically air. Gas-side resistance then exists, but usually contributes to only a few percent of the total resistance. Its impact can be taken into account if known from independent measurements or from appropriate literature correlations, a frequently applied option, or, if the system is in the intermediate regime, by using a variant of Danckwerts' plot.<sup>12</sup>

**Danckwerts' Plot (Intermediate Reaction Regime): Methodology.** If the reaction is in the intermediate reaction regime, that is, the condition  $E > 9$  or  $E > 5$  is not met, then the so-called Danckwerts' plot method can be used. Studies using this approach are listed in Table 2. The approximation of  $E$  as  $E = \sqrt{(1 + \text{Ha}^2)}$  leads to the following expression for the volumetric flux of solute:

$$\Phi = k_L a_e A^* \sqrt{1 + \frac{D_A k_R}{k_L^2}} \quad (26)$$

which can be squared to give:

$$\Phi^2 = (k_L a_e A^*)^2 + D_A (a_e A^*)^2 k_R \quad (27)$$

The Danckwerts' plot then shows  $\Phi^2$  against  $k_R$  as a straight line, with  $(k_L a_e A^*)^2$  as the intercept and  $(a_e A^*)^2 D_A$  as the slope which then yield  $k_L$  and  $a_e$ . The reaction rate  $k_R$  can be varied by either changing the concentration of  $B$  or of a catalytic agent. The use of a catalyst has the advantage of keeping constant the physical properties of the system. A version of the method can be applied even if the gas-side resistance is not negligible.<sup>13,42</sup> The uncertainty of the intercept is always greater than that of the slope, so the error of  $k_L$  is higher than that of  $a_e$ .

**Chemical System.** Systems for the intermediate reaction regime include the absorption of CO<sub>2</sub> into sodium or potassium bicarbonate buffer solutions, with either NaOCl or KAsO<sub>2</sub> as catalysts (Table 2). Danckwerts and Sharma<sup>64</sup> also mentioned formaldehyde as potential catalyst. The catalyst concentration is varied to create the Danckwerts' plot. Jhaveri and Sharma<sup>29</sup> noted that under certain conditions, the reaction of O<sub>2</sub> and CuCl can fall in this regime as well. The work of Rizzuti<sup>37,61,62</sup> applied a potassium bicarbonate buffer with

**Table 3. Main Details of Other Methods Using Chemical Absorption to Determine  $a_e$**

Source	Packing	Gas	Liquid	Principle
Danckwerts and Gillham <sup>60</sup>	Raschig rings	Pure CO <sub>2</sub> (saturated with water vapor)	K <sub>2</sub> CO <sub>3</sub> + KHCO <sub>3</sub> + NaOCl (aq) NaOH + Na <sub>2</sub> SO <sub>4</sub> (aq) Na <sub>2</sub> SO <sub>4</sub> (aq) NaOH (aq)	Analogy with stirred cell
Benadda et al. <sup>24</sup>	Berl saddles	CO <sub>2</sub> in N <sub>2</sub>	NaOH (aq)	Regressed as model parameter
Nakov <sup>68</sup>	Honeycomb	NH <sub>3</sub>	H <sub>2</sub> SO <sub>4</sub> + sugar (aq)	Gas-film control, comparison with complete wetting
Aroonwilas and Veawab <sup>25</sup>	Sulzer DX	CO <sub>2</sub> in N <sub>2</sub>	various amines	Regressed as model parameter

KAsO<sub>2</sub> in a the packed column operated without gas outlet. This is a convenient method to measure the amount of absorbed gas, as it will be equal to the inlet gas flow, however, it assumes that the gas flow rate has no effect on  $a_e$ . Several investigators consider this assumption to be valid below the flooding point.<sup>2</sup> Others indicate that the gas flow rate may have an effect (e.g., Weisman and Bonilla<sup>65</sup>; Nakajima et al.<sup>44</sup>; Alix et al.,<sup>53</sup> the correlations of Shulman et al.<sup>66</sup> and Bravo and Fair<sup>67</sup>).

### Other methods

In this section, less common chemical absorption methods are briefly reviewed as listed in Table 3.

Danckwerts and Gillham<sup>60</sup> used the stirred cell by analogy to a packed column with pure CO<sub>2</sub> to remove gas-side resistance. In the stirred cell, gas is absorbed into the liquid through a known flat interfacial area given by the horizontal cross-section of the cell. The validity of this analogy assumption was later verified with a maximum uncertainty of 14% by a first-order reaction method. Gas continuously flows through the cell while the liquid may or may not be renewed. The stirrer is positioned such that the bottom edge of the blades skims the liquid surface. The authors made absorption measurements both into reacting and into CO<sub>2</sub>-free inert solutions. The ratio of the absorption rates:

$$\gamma_{DG} = \frac{\text{Rate of absorption into reacting solution}}{\text{Rate of absorption into CO}_2\text{-free inert solution}} = \frac{Ek_L(A^* - A^0)}{k_L A^*} \quad (28)$$

is evaluated for the cell as a function of stirring speed. The chemical systems used, bicarbonate buffer or NaOH, ensured that  $A^0$ , the concentration of CO<sub>2</sub> in the bulk liquid, was null

leading to a common absorption driving force  $A^*$  in the numerator and denominator of Eq. 28 such that  $\gamma_{DG}$  becomes equal to  $E$ . The value of  $E$  depends on  $k_L$  and on the nature of the reactive solution. The authors therefore assumed that when the cell and the column have equal values of  $E$ , then they also have equal values of  $k_L$ . For a given stirring speed,  $k_L$  was calculated for the cell by knowledge of its interfacial area. The liquid flow rate of the packed column was then varied to obtain the same  $E$ . Under this condition,  $a_e$  can be calculated by dividing the volumetric mass-transfer coefficient  $k_L a_e$  with the  $k_L$  of the cell. The calculation procedure is illustrated in Figure 4.

The method of Nakov<sup>68</sup> differs fundamentally from those presented above. The system, absorption of NH<sub>3</sub> into sulfuric acid is gas-side controlled. The method is based upon the fact that in this case, the effect of liquid flow rate on  $k_G$  is negligible at low values of liquid superficial velocities. By further assuming that the packing is completely wetted above a given liquid flow rate,  $a_e$  can be calculated from:

$$\frac{a_e}{a_g} = \frac{k_G a}{(k_G a)_L} \quad (29)$$

where  $(k_G a)_L$  is the volumetric mass-transfer coefficient at the liquid superficial velocity corresponding to completely wetted packing. The drawback of the method is that it implicitly assumes that the absorption occurs only on the surface of the packing, and not in liquid elements between packings.

Recent approaches to determine  $a_e$  consist in developing more complete models of packed columns than the simpler expressions relating the global measured concentrations to the global mass transfer parameters. With these models, the parameter  $a_e$  is determined by varying its value to match the calculated solute concentrations to the experimental ones.<sup>24,25</sup>

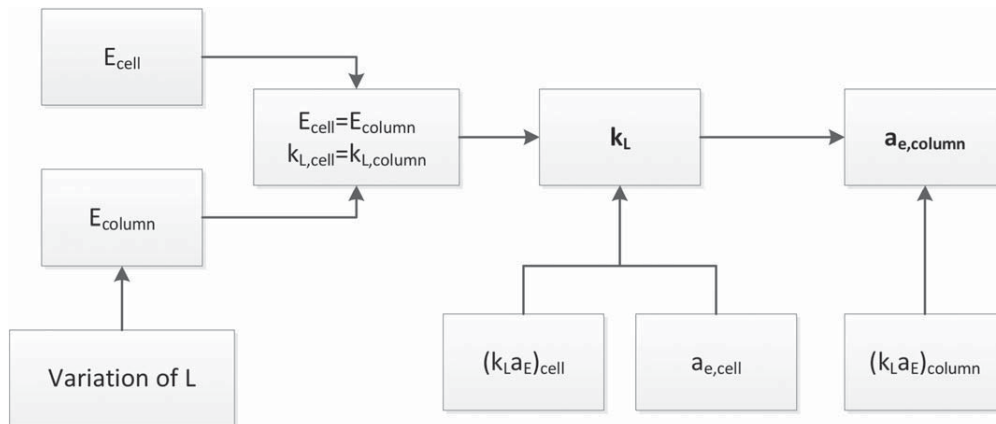


**Figure 4. The calculation procedure of Danckwerts and Gillham<sup>60</sup> for the determination of  $a_e$  and  $k_L$ .**

**Table 4. Main Details of the Methods Using Physical Absorption to Determine  $a_e$** 

Source	Packing	Gas	Liquid	Principle
Yoshida and Koyanagi <sup>73</sup>	Raschig rings, Berl saddles, spheres	Pure CO <sub>2</sub> (saturated with absorbent)	Water Methanol	Analogy with bead column
Hikita et al. <sup>74</sup>	Raschig rings, Berl saddles	Pure CO <sub>2</sub>	Water Sugar (aq) Methanol (aq) Methanol	Analogy with single piece of packing
Yoshida and Koyanagi <sup>71</sup>	Raschig rings	Methanol in air	Water	Comparison with packed column of fully wetted packing

The model of Benadda et al.<sup>24</sup> takes the effect of axial dispersion into account. The rigorous model of Aroonwilas and Veawab<sup>25</sup> accounts for heat of absorption, solvent evaporation, and simultaneous heat and mass transfer. Rejl et al.<sup>69</sup> proposed a “profile method,” where not only inlet and outlet concentrations, but also the concentration profiles are compared to the model results, although it was applied only for distillation. These methods allow relaxing experimental operating constraints required for the simpler “ideal” systems and open up alternatives. A small disadvantage of this method is that a more complex model has to be developed or adapted.

### Evaporation

The method using evaporation (vaporization) of a pure liquid to determine  $a_e$  compares the volumetric mass-transfer coefficient  $k_G a_e$  measured in a packed column to that measured in a second packed column filled with a packing of the same geometry but made of a porous material to ensure complete wetting. It assumes that the values of  $k_G$  are equal if the packings and the experimental conditions are identical. The wetted area of the porous packings equals the geometric area  $a_g$  and allows to calculate  $k_G$ . The unknown  $a_e$  of the first column, which will be smaller than the  $a_g$  due to incomplete wetting, is then obtained by dividing the measured volumetric mass-transfer coefficient by  $k_G$ . Weisman and Bonilla<sup>65</sup> used spheres as packing, and compared their results to those of Gamson et al.<sup>70</sup> under the same Reynolds number ( $Re_G$ ) and liquid flow rate. Yoshida and Koyanagi<sup>71</sup> applied the technique with Raschig rings, and made comparisons to data from Taecker and Hougen,<sup>72</sup> by assuming that  $k_G$  values were identical in the two columns for the same Reynolds ( $Re_G$ ) and Schmidt ( $Sc_G$ ) numbers. The packings of Taecker and Hougen<sup>72</sup> were made of a special clay-kieselguhr mixture having high porosity and capillarity, thus ensuring complete wetting. Both Gamson et al.<sup>70</sup> and Taecker and Hougen<sup>72</sup> applied water flow only to saturate the packings with water and then varied the air flow rate to measure  $k_G a_e$ . Since in this case liquid was present only on the surface of the packings, the effective interfacial area was equal to the known wetted area.

This method can determine the effective area which equals the interfacial area for an evaporation process. The necessity to first measure the  $k_G$  and to apply special, custom-made packings is clearly penalizing particularly in the case of thin structures.

### Physical absorption

The methods relying on physical absorption of a gas constituent in a liquid calculate the effective area by dividing the volumetric mass-transfer coefficient with either  $k_G$  or  $k_L$ . The value of the latter must first be determined by measuring the volumetric mass-transfer coefficient in another apparatus

having a well-defined effective interfacial area under conditions that ensure the equality of  $k_G$  or  $k_L$  between the two apparatus. Meeting this last constraint is the main difficulty. In the case of chemical absorption, it was reached by matching the enhancement factor  $E$  as presented earlier in Figure 4. The other apparatus can be a packed column with fully wetted packings, as in the case of evaporation (sections “Determination of the Effective Interfacial Area—Evaporation” and “Determination of the Effective Interfacial Area—Physical absorption—Comparison to a packed column with fully wetted packing”), or a device with largely different hydrodynamics in which case, the term “analogy” is used to describe the methodology (section “Determination of the Effective Interfacial Area—Physical absorption—Analogy between a packed column and another apparatus”). The articles using the method of physical absorption are listed in Table 4.

*Comparison to a Packed Column with Fully Wetted Packing.* The determination of  $a_e$  by comparing two packed columns one of which has a fully wetted packing was applied by Yoshida and Koyanagi<sup>71</sup> with both vaporization (section “Determination of the Effective Interfacial Area—Evaporation”) and physical absorption. The mass-transfer coefficient  $k_G$  was used for the analogy. Methanol vapor was absorbed from air into water with Raschig rings as packing, and the results were compared to those of Taecker and Hougen<sup>72</sup> at the same  $Re_G$  and  $Sc_G$ , as described in the section “Determination of the Effective Interfacial Area—Evaporation.” With this procedure, the effective interfacial area of the given process (evaporation or physical absorption) is obtained. The disadvantage is the need for a special porous packing of the same geometry.

*Analogy Between a Packed Column and Another Apparatus.* The principle of the method of analogy is that even though the other apparatus may be significantly different from a packed column, if the conditions of the analogy are met, which means the equality of one or more parameters, the mass-transfer coefficients will be equal. Two types of devices have been used for this type of analogy (Table 4), one consisting of a single piece of packing,<sup>74</sup> and the other of a bead column.<sup>73</sup> The gas phase was pure CO<sub>2</sub> in both papers, meaning that there is no resistance in the gas film, and the coefficient  $k_L$  was used for the analogy. Different liquids were applied to study the influence of physico-chemical properties on mass transfer parameters. In Hikita et al.,<sup>74</sup> who used a single piece packing with known surface,<sup>75</sup> the condition of analogy was the equality of liquid-side Reynolds numbers. The bead column is a vertical row of spheres, drilled through and connected by a stainless steel wire. The spheres are separated by short distances, and their surface is considered to be fully wetted. According to Yoshida and Koyanagi,<sup>73</sup> three parameters have

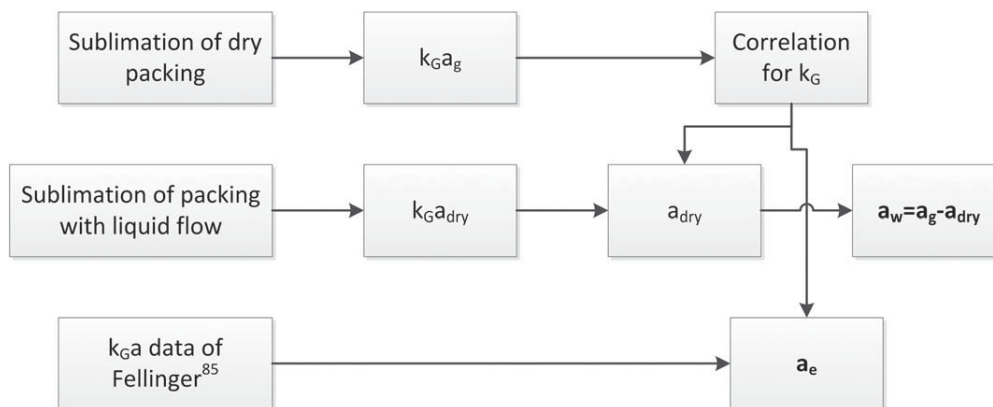


Figure 5. Calculation procedure to determine  $a_w$  and  $a_e$  with the method of the sublimation of the packing.

to be identical for the equality of  $k_L$ : (1)  $Re_L$  is based on the effective part of the liquid stream, (2) the number of times and degree of mixing of liquid streams, (3) the distance travelled over each packing piece by the liquid. Conditions 2 and 3 are fulfilled if the spheres of the bead column have the same size as the packing elements in the packed column, and the number of spheres equals the calculated number of packing pieces in the vertical direction of the packed column. The liquid flow rates of the two columns are adjusted so as to have the same number of transfer units, and according to the assumption, the same  $Re_L$ . For both columns,  $Re_L$  includes the effective wetted periphery, which contains the unknown  $a_e$  for packed column, but which is known from the sphere size for the bead column. An expression for  $a_e$  can be derived from the equality of Reynolds numbers.

The method of analogy can determine the effective interfacial area of physical absorption, but its disadvantage is that another apparatus is required, and the validity of the analogy has to be checked before applying the method.

### Tomography

A new and promising method is the application of tomography, which makes it possible to visualize the inside of a column even under operation. Although tomography has been used to study packed columns, for example, to determine liquid hold-ups or observe gas and liquid distribution,<sup>76</sup> to the best of our knowledge, the method has only been applied for the determination of the wetted area in two research groups at the University of Texas at Austin<sup>49,77</sup> and at the Université de Liège.<sup>54,78</sup> Both groups used x-rays that are capable of passing through metal sheets and of providing a spatial accuracy of around 300  $\mu\text{m}$ . Air and water were used on Mellapak 250.Y and 500.Y packings in the case of Green, and on Katapak SP2 and Mellapak 752.Y in the case of Aferka. The column was rotated while the x-ray source and detectors were fixed. There is no mention to what extent the rotation alters the flow patterns and the value of the wetted area. Green determined the wetted area by setting a threshold greyscale value for pixels, so that the calculated iso-surface would be the surface separating the gas and liquid phase. Aferka counted the pixels containing liquid in contact with the gas phase. The results of both authors were reported to agree with values of  $a_e$  obtained by chemical absorption method within less than 3%.

As compared to other methods that measure the wetted area, x-ray tomography provides a more physical evaluation

since it is based on a visualization technique. The uncertainty limit is determined by the resolution of the tomograph. The equipment for using this method is however not readily accessible to researchers owing to high costs and requirements for dedicated scanning bay with containment walls to shield radiation.

### Colorimetry

In this method, a dye is added to the liquid phase that will color the packing surfaces with which it comes into contact. The wetted area is simply determined by measuring the total dyed surface. The method was first used by Mayo et al.,<sup>79</sup> which is also among the very first papers dealing with the determination of interfacial area in packed columns. Paper-made Raschig rings were used as packing material. The method was later applied by several Japanese authors,<sup>80,81</sup> including Onda et al.<sup>82</sup> and Choi and Kim<sup>83</sup> used both ceramic and paper-made Raschig rings. The problem with colorimetry is that it leads to overestimated wetted areas due to fluctuations of the liquid flow pathways that generate a dyed packing surface that is greater than the instantaneous wetted area. Moreover, the wettability of paper is different than for the material of commercial packings. The method is not convenient experimentally as it requires changing the bed at every condition and making visual evaluations of the dyed areas. Finally, its application to packing materials other than ceramic is uncertain.

### Packing sublimation

The sublimation of the packing is a method that was used by the group of Shulman.<sup>20,84</sup> The packings (Raschig rings and Berl saddles) were specially made from naphthalene, and they were sublimated into a gas stream, first without the presence of liquid phase, and then under different water flow rates.

Figure 5 presents the process to calculate  $a_w$  and  $a_e$ . By measuring the concentration in the outlet gas,  $k_G a_g$  is determined, since the entire surface of the packing is sublimating. If the measurement is performed at various gas flow rates, and by knowing the value of  $a_g$ , a correlation for  $k_G$  can be obtained. When the experiments are repeated with liquid flow sublimation takes place only on the dry surfaces. The correlation for  $k_G$  then allows calculating the dry area, and the wetted surface area is obtained by difference with the total area. This calculation method assumes that the presence of the liquid phase does not change the nature of the gas flow. Finally, it is

possible to determine  $a_e$ , from volumetric mass-transfer coefficients measured by absorption (or vaporization) with the assumption that the  $k_G$  values of the sublimation and absorption experiments are identical under the same operating conditions. Shulman uses the volumetric mass-transfer coefficients of Fellingner<sup>85</sup> measured by absorption of ammonia into water.

The sublimation method can determine the wetted surface area and since it gives  $k_G$ , it can indirectly allow deriving the effective surface area of an arbitrary gas–liquid mass transfer process. However, it requires custom-made packings, which greatly impedes its use, especially if we consider thin structured or modern random packings, and the wettability may not be representative. Moreover, the parameter  $k_G$  is assumed to be independent of liquid load.

### Conclusion

A variety of methods with different measurement principles are described in the literature for the determination of gas–liquid interfacial area in packed columns. As there are different concepts of interfacial area, such as wetted and effective interfacial area, and because the value of effective interfacial area depends on the nature of the mass transfer process, it is important to be aware what each method measures. This information is given in Table 5.

The method of chemical absorption can determine the effective interfacial area, which may be equal to the interfacial area, provided that the rate of absorption does not locally lead to saturation of the liquid phase. The most popular method is to use a fast, irreversible pseudo-first order reaction, most often that of  $\text{CO}_2$  and  $\text{NaOH}$ , with negligible resistance in the gas phase, as under these conditions, the mass transfer rate becomes independent of  $k_L$ , and the interfacial area can be directly calculated. For the successful use of this method, one has to know the kinetics of the reaction, the physical properties of the system, and verify that the system is under appropriate fast reaction regime over the full range of conditions covered in the experiments. The system using  $\text{CO}_2$  absorption (from air) into dilute  $\text{NaOH}$  solutions which meets the required constraints over a wide range of operating conditions and packing materials, making it a recommended method. A further advantage is that the reactants are readily available with little innuocuity.

Methods based on physical absorption and vaporization of pure liquids require analogy to other apparatus, or comparison with another packed column using fully wetted packings. The validity of analogy is a critical issue to determine whether or not the results will be accurate. They further can require preparing porous, fully wetted alternatives of packings, which is either cumbersome or impossible, therefore these methods are not recommended. Colorimetry or packing sublimation is not recommended either as the former overestimates  $a_w$  while the latter requires special packings. A new and promising method is tomography, which allows determining  $a_i$  directly. However, it requires sophisticated equipment.

**Table 5. Types of Area Measured by Different Methods**

Method	Area
Chemical absorption	$a_e (\leq a_i)$
Vaporization	$a_e = a_i$
Physical absorption	$a_e = a_{\text{dyn}}$
Tomography	$a_w$
Colorimetry	$a_w$
Sublimation	$a_w, a_e$

### Determination of the Gas-Side Mass-Transfer Coefficient

All methods described in the literature provide a column averaged volumetric mass-transfer coefficient  $k_G a$ . Local values of  $k_G$  cannot be determined directly as techniques for measuring local concentrations in the gas or liquid film are not currently available. In many cases, the liquid-side mass transfer resistance is negligible in which case the process is controlled solely by  $k_G a$ . In theory, this condition holds only when the liquid phase is a pure substance. In every other situation, liquid-side resistance is more or less present, to an extent that depends on the system and on the gas and liquid flow rates. As discussed earlier (section “Determination of the Effective Interfacial Area—Specific areas defined in packings”),  $k_G$  can be calculated if  $a_e$  is known for the type of mass transfer process with which  $k_G a_e$  was obtained. For example, a vaporization process will need  $a_i$ , whereas a physical absorption process where stagnant liquid areas may be saturated requires  $a_{\text{dyn}}$ . The methods for determining the gas-side mass-transfer coefficient can be classified into the following groups based on the principle of the measurement:

- vaporization of a pure liquid,
- physical absorption (and desorption),
- chemical absorption.

In the next sections, the methods found in the literature are presented, and the advantages and drawbacks of each group of methods are discussed.

#### Vaporization

In this method, a pure liquid is vaporized into a gas stream, and since no liquid-side resistance exists, it may seem to be a straightforward choice. The column should operate close to the state of adiabatic saturation in order to minimize the temperature gradients generated from the evaporative cooling of the liquid phase as these will significantly affect the interfacial vapor partial pressures that control the mass transfer driving force. In the majority of the experiments, this state is achieved by recirculating the liquid, and performing the measurement when its temperature is sufficiently stable in which case it is close to the adiabatic saturation temperature. An alternative<sup>71,86,87</sup> consists in modifying the temperature of the inlet liquid to minimize the temperature difference between the inlet and the outlet. Another problem with the method is that the height of packed bed by which vapor saturation is reached in the gas phase is relatively short,<sup>88</sup> because  $k_G a$  is high relative to the gas superficial velocity at the operating conditions commonly used. When saturation is approached, the results become more sensitive to measurement errors due to increased uncertainties in evaluating the driving force at the top of the column. However, with shorter packed beds, the contribution of the end-effects becomes more pronounced as the gas and liquid distribution within the packings may not have time enough to become fully established and representative of those in industrial columns.

The studies that have applied the method of vaporization are listed in Table 6. The method was particularly popular in the 40s and 50s. The gas phase was air in the majority of cases with some exceptions where He,  $\text{CO}_2$ , or Freon-12 (dichlorodifluoromethane) were used to study the effect of the physical properties of the gas. In some investigations where the gas was not air, it was recirculated<sup>87,93</sup> with partial moisture removal by condensation. An initial moisture content can be advantageous, as it prevents from reaching a low adiabatic

**Table 6. Main Features of the Methods Using the Vaporization of a Pure Liquid to Determine  $k_G$**

Source	Packing	Gas	Liquid (pure constituents)
Sherwood and Holloway <sup>88</sup>	Raschig rings	Air	Water Methanol Benzene Toluene
Van Krevelen et al. <sup>89</sup>	Rings, spheres	Air	Water
McAdams et al. <sup>90</sup>	Raschig rings	Air	Water
Surosky and Dodge <sup>91</sup>	Rings	Air	Water Methanol Benzene Ethyl n-butanoate
Weisman and Bonilla <sup>65</sup>	Spheres	Air	Water
Yoshida and Tanaka <sup>92*</sup>	Raschig rings	Air	Water
Hensel and Treybal <sup>86</sup>	Berl saddles	Air	Water
Lynch and Wilke <sup>87</sup>	Raschig rings	Air He Freon-12	Water
Yoshida <sup>93</sup>	Raschig rings	Air He CO <sub>2</sub>	Water
Shulman and Delaney <sup>94</sup>	Raschig rings	Air + CCl <sub>4</sub>	CCl <sub>4</sub>
Shulman and Robinson <sup>95*</sup>	Raschig rings	Air + CCl <sub>4</sub>	CCl <sub>4</sub>
Yoshida and Koyanagi <sup>71</sup>	Raschig rings	Air	Water
Shulman et al. <sup>21</sup>	Raschig rings	Air	Water
Vidwans and Sharma <sup>28</sup>	Raschig rings	Air He Freon-12	Triethylamine
Onda et al. <sup>96</sup>	Raschig rings, Berl saddles, spheres	Air	Water
Alix et al. <sup>53</sup>	4D	Air	Water

\*Partially or entirely dehumidification.

saturation temperature and reduces undesired heat transfer with the environment. In cases where the gas phase was air, it was generally drawn directly from the atmosphere. In some studies, the air was actually dried before entering the column while in others<sup>53</sup> the air was actually humidified by water evaporation in a preheater.

The evaporated liquid has usually been water as it is the simplest option. A number of organic liquids have been used as well. Sherwood and Holloway<sup>88</sup> and Surosky and Dodge<sup>91</sup> studied the effect of vapor diffusivity on  $k_{Ga}$  and found a power law dependency of  $D^{0.17}$  and  $D^{0.15}$ , respectively. The values of these exponents are much lower than those generally proposed by correlations for  $k_G$  which range between 1/2 and 2/3.<sup>2</sup> Sherwood and Holloway<sup>88</sup> and Surosky and Dodge<sup>91</sup> concluded that eddy diffusivity plays an important role in establishing the gas-side mass transfer rate, but they did not consider the effect of liquid properties on  $a_c$  (especially surface tension), which may have led to underestimated diffusivity exponents. Shulman and Delaney<sup>94</sup> vaporized CCl<sub>4</sub> into air already containing the substance at different concentration levels in order to study the effect of  $p_{BM}$ , the mean partial pressure of the inert carrier gas. In addition, using CCl<sub>4</sub> instead of water makes it possible to obtain more generally valid correlations, as the physical properties of the gas phase change to a greater extent with concentration.<sup>95</sup> For example,  $Sc_G$  shows a fivefold variation with CCl<sub>4</sub> mole fraction ranging from 0 to 0.7 in air.

The mass transfer driving force includes the equilibrium concentration of the liquid constituent in the gas phase at the adiabatic saturation temperature, which is assumed to be the liquid temperature. The precision of the temperature measurement is therefore critical for determining the  $k_{Ga}$ : a 1°C difference at 20°C causes a 6% change in the vapor pressure of water. If the system is within 20% of saturation, this can represent a 30% uncertainty in  $k_{Ga}$ . If the liquid phase is other than

water, chemical analysis of the gas phase is required, instead of the simpler humidity measurement.

The reverse process, dehumidification, or condensation, has also been used as a method for determining  $k_{Ga}$ . Yoshida and Tanaka<sup>92</sup> and Shulman and Robinson<sup>95</sup> performed such tests, where the solute content of air was reduced by getting it into contact with a cold liquid stream, thus partially condensing the vapor. The correlations established for vaporization can only be applied here with a precise measurement or a rigorous estimation<sup>95</sup> of interfacial temperature. With dehumidification, the temperature of the liquid surface differs from that of the bulk liquid, as heat transfer takes place in the liquid, unlike the case of constant liquid temperature vaporization, where the constant liquid temperature means that vaporization heat is provided entirely by the gas phase.<sup>92</sup> For this reason, dehumidification is not a practical alternative to vaporization.

Vaporization of a pure liquid, especially if air and water are used, is a practical method to determine  $k_{Ga}$ . The liquid phase offers no resistance, and if the liquid is water, only the temperature and humidity measurements are needed with no use of other chemicals or chemical analysis. However, the water temperature stability must be ensured, preferably within  $\pm 0.2^\circ\text{C}$ , in order to minimize the heat transfer in the liquid phase and resulting uncertainties in the evaluation of the driving force. Moreover, the packed bed height must be kept low enough to avoid getting close to saturation which otherwise also induces driving force uncertainties.

### Physical absorption

The method of physical absorption relies on using a solute of very high solubility in the liquid so as to minimize liquid-side resistance and sensitize the absorption flux only to the gas side mass-transfer coefficient. In most cases, the liquid-side resistance, although low, is not negligible, which requires some means of assessing its value in order to calculate  $k_{Ga}$ .

**Table 7. Main Characteristics of the Methods Using Physical Absorption to Determine  $k_G$**

Source	Packing	Gas	Liquid	Method
Dwyer and Dodge <sup>105</sup>	Raschig rings	NH <sub>3</sub> in air	Water	$k_L a_e$ subtracted from $K_G a_e$
Othmer and Scheibel <sup>102</sup>	Raschig rings	Acetone in air	Water	Assumption 1 + 2
White and Othmer <sup>103</sup>	Stedman triangular pyramid	Acetone in air	Water	Assumption 1 + 2
Molstad et al. <sup>107</sup>	Raschig rings, Berl saddles, spiral rings, partition rings, drip-point ceramic grids, wood grids	NH <sub>3</sub> in air	Water	$k_L a_e$ subtracted from $K_G a_e$
Scheibel and Othmer <sup>104</sup>	Raschig rings	Acetone in air	Water	Assumption 1 + 2
Gross and Simmons <sup>106</sup>	Berl saddles	Butanone in air Benzene in air Trichloroethylene in air Chloroform in air	Kerosene	Liquid-side resistance was neglected
Van Krevelen et al. <sup>89</sup>	Rings, spheres	NH <sub>3</sub>	Water	Assumption 1 + 2
Landau et al. <sup>108</sup>	Raschig rings	NH <sub>3</sub> in N <sub>2</sub> UF <sub>6</sub> in N <sub>2</sub>	Water Heavy oil	$k_L a_e$ subtracted from $K_G a_e$ Assumption 1
Hutchings et al. <sup>109</sup>	Raschig rings	Acetone in air	Water	Assumption 1 + 2
Whitney and Vivian <sup>99</sup>	Raschig rings	SO <sub>2</sub>	Water	Assumption 1
Molstad and Parsly <sup>110</sup>	Drip-point ceramic grids	NH <sub>3</sub> in air	Water	$k_L a_e$ subtracted from $K_G a_e$
Houston and Walker <sup>111</sup>	Raschig rings	NH <sub>3</sub> in air Acetone in air Methanol in air Ethanol in air	Water	$k_L a_e$ subtracted from $K_G a_e$
Zabban and Dodge <sup>112</sup>	Raschig rings, Berl saddles	Acetone in air Methanol in air	Water	$k_L a_e$ subtracted from $K_G a_e$
Onda et al. <sup>113</sup>	Raschig rings, Berl saddles, spheres	NH <sub>3</sub> in N <sub>2</sub>	Water	$k_L a_e$ subtracted from $K_G a_e$
Yoshida and Koyanagi <sup>71</sup>	Raschig rings	Methanol in air	Water	Liquid-side resistance was neglected
Shulman et al. <sup>21</sup>	Raschig rings	Methanol in air	Water	$k_L a_e$ subtracted from $K_G a_e$
Billet and Maćkowiak <sup>114</sup>	Pall, Impulse type 50	NH <sub>3</sub> in air	Water	$k_L a_e$ subtracted from HTU <sub>OG</sub>
Maćkowiak <sup>115</sup>	Mellapak 250.Y, Montz B1, C1, Gempak 2A	NH <sub>3</sub> in air	Water	$k_L a_e$ subtracted from HTU <sub>OG</sub>
San-Valero et al. <sup>116</sup>	Flexiring, PAS Winded Media	Isopropanol in air	Water	Liquid-side resistance was neglected

The relative magnitude of the two resistances also depends on the flow conditions for which a high  $L/G$  value is preferred to minimize the liquid-side resistance.

Literature sources use different approaches to obtain  $k_G a_e$  from the overall coefficient  $K_G a_e$ . A common method consists in measuring independently the liquid-side resistance or estimating it with a correlation, and then subtracting it from the total mass transfer resistance. Numerous authors apply assumptions on the dependence of  $k_G a_e$  and  $k_L a_e$  on gas and liquid flow rates ( $G$  and  $L$ , respectively) to assess evolutions of their relative contributions with flow conditions. The independency of  $k_L a_e$  to  $G$  (Assumption 1) is generally accepted to be true below the loading point. According to penetration theory,  $k_L a_e$  does not depend on  $G$ . This has been confirmed experimentally such that the values of  $k_L a_e$  recalculated from the correlations reviewed by Wang et al.<sup>2</sup> for  $k_L$  and  $a_e$  are independent of the gas flow rate. The experimental work of Murrieta et al.<sup>97</sup> showed that  $k_L a_e$  did not change by varying  $G$  below the loading point, although Sherwood and Holloway<sup>98</sup> found an increase in the loading region. It is also known that  $a_e$  becomes dependent on  $G$  above the loading point. On the basis of the above, the gas-side total resistance can then be expressed as:

$$\frac{1}{K_G a_e} = \frac{1}{k_G a_e} + \frac{m}{k_L a_e} = \frac{1}{\beta G^q L^p} + \frac{m}{\alpha L^p} = \frac{m}{K_L a_e} \quad (30)$$

Whitney and Vivian<sup>99</sup> applied this equation, to determine and establish correlations for both  $k_G a_e$  and  $k_L a_e$ . This was done by plotting  $1/K_L a_e$  against  $1/G^q$  at constant liquid flow rate.

The value of the exponent  $q$  was optimized to get the best linear fit. Repeating the procedure for several values of  $L$ , the intercepts ( $1/\alpha L^p$ ) and slopes ( $1/m\beta L^p$ ) of the lines were then plotted as a function of  $L$ , to determine the exponents  $p$  and  $r$ .

Several authors have assumed that the exponent  $q$  equals 0.8 (Assumption 2). This value was chosen on the basis of wetted-wall column investigations, and the work of Sherwood<sup>100</sup> who correlated the data of Kowalke et al.<sup>101</sup> The overall mass transfer resistance is then:

$$\frac{1}{K_G a_e} = \frac{1}{\beta G^{0.8}} + \frac{m}{k_L a_e} \quad (31)$$

If  $1/K_G a_e$  is measured at different gas flow rates and plotted against  $1/G^{0.8}$ , then the parameter  $\beta$  can be determined from the slope of the resulting straight line, leading to a correlation for  $k_G a_e$  in the form of  $k_G a_e = \beta G^{0.3}$ . The liquid-side resistance can be calculated from the intercept. This method was used by the group of Othmer<sup>102–104</sup> and by Van Krevelen et al.<sup>89</sup> for the separation of the gas- and liquid-side resistances.

The coefficient  $\beta$  can encompass the eventual dependence of  $k_G a_e$  on  $L$ , as long as the measurements are performed at a constant  $L$ . If data at different liquid flow rates are used for the same line then  $k_G a_e$  is assumed independent of  $L$ . Several authors (e.g., Dwyer and Dodge<sup>105</sup>) indicate however that this assumption does not hold, because  $L$  can increase  $k_G a_e$  by increasing turbulence in the gas film.

The validity of Assumption 2 is questionable as numerous other measurements have led to exponent values ranging between 0.5 and 1.<sup>2</sup> If the measurement points do not fall on a

line, it would indicate that the exponent is different from 0.8, but taking into account the measurement errors the conclusions are not trivial.

Gross and Simmons<sup>106</sup> neglected liquid-side resistance on the basis that none of the parameters of the equation

$$K_G a_e = \alpha G^{\gamma} \quad (32)$$

seemed to depend on the liquid flow rate.

Table 7 lists the main experimental characteristics of articles using the physical absorption method along with assumptions for treating the data. The method was popular up into the 60s; with the first experiments performed in the 40s.

In some cases,<sup>21,99,105</sup> the gas phase was humidified before entering the absorption column. This measure was taken to reduce any unwanted temperature drop from water evaporation in the absorption column, which would alter the measured  $k_G a_e$ . The evaporation of water can also directly hinder the diffusion of the solute, which proceeds in the opposite direction. The only author to investigate the measurement error caused by the water evaporation was Dwyer and Dodge<sup>105</sup> who found the overall mass-transfer coefficient to be lower if the gas was humidified, but in most cases the difference fell within experimental uncertainty.

The various solutes have been  $\text{NH}_3$ , organic solvents, such as acetone, methanol, ethanol, and isopropanol, or in one case,<sup>99</sup>  $\text{SO}_2$ , and they were mixed to a carrier gas, air, or  $\text{N}_2$ . The concentrations of solute in the inlet gas, when given, have generally ranged between 1 and 10 mol%. Lower values down to 0.12 mol% can be found in Scheibel and Othmer<sup>104</sup> and higher values up to 25 mol% have been used by Gross and Simmons,<sup>106</sup> Hutchings et al.<sup>109</sup>, and Whitney and Vivian.<sup>99</sup> In the case of  $\text{NH}_3$  absorption, Whitney and Vivian<sup>99</sup> specifically warned that although some authors neglected the liquid-side resistance, its contribution may be significant, sometimes reaching half of the total resistance at low  $L/G$  values. The liquid phase has generally been water, with the exception of Gross and Simmons<sup>106</sup> and Landau et al.<sup>108</sup> The latter investigated extreme conditions in terms of density, viscosity, diffusivity of the fluids using  $\text{UF}_6$  absorption into a heavy oil (molar masses: 352 and 750 g/mol, respectively) at temperatures around 90°C in order to assess the extrapolability of correlations for design and calculation methods. Good agreement was obtained between experimental results and the values calculated using correlations for  $k_G a$  and  $k_L a$  (corrected for the changed physical properties). The authors used desorption data from the same system, as well.

The method of physical absorption has the advantage that no chemical reaction takes place, and that saturation of the liquid phase is usually not a problem. However, a fundamental problem is the existence of liquid-side resistance, the contribution of which should be assessed for every flow condition. In some cases, it may very well be negligible, but more often than not the liquid-side resistance in these systems has an impact that is increasingly important at lower values of  $L/G$  where  $k_L a$  is smaller. When both resistances contribute significantly to the overall mass transfer rate, then  $k_G a$  can be extracted from the data simultaneously with  $k_L a$  provided that assumptions are made on the dependency of these parameters on  $G$  and  $L$  or that  $k_L a_e$  can be independently evaluated by other means (experimental, correlations). When the liquid-side resistance is secondary to the overall resistance, the uncertainties in estimating  $k_L a_e$  will not significantly affect the determined  $k_G a_e$  values.

## Chemical absorption

The liquid-side resistance can be eliminated or greatly reduced by a chemical reaction rapidly consuming the solute such that  $K_G a_e = k_G a_e$ , and  $k_G$  can be calculated by dividing with  $a_e$ . The reaction can be instantaneous or of finite speed, but must be very fast in order to eliminate the solute from the liquid film, and thus the liquid-side resistance.<sup>12</sup> The necessary condition for an instantaneous reaction is<sup>13</sup>:

$$\text{Ha} \gg E_{\text{inf}} \quad (33)$$

Danckwerts and Sharma<sup>64</sup> states that a 10-fold difference between  $\text{Ha}$  and  $E_{\text{inf}}$  is sufficient.

The reaction plane is the location in the liquid film where the instantaneous reaction takes place. If the following additional condition also holds:

$$k_G p < k_L \frac{D_A B^0}{D_B v} \quad (34)$$

then the reaction plane is at the interface which eliminates the liquid-side resistance. In the above expression,  $p$  is the partial pressure of the solute in the bulk gas phase. Sharma and Danckwerts<sup>12</sup> specify the above condition in the following forms for  $v = 1$ :

- for an instantaneous reaction by assuming equal diffusivities:

$$k_G p < k_L B^0 \quad (35)$$

- for a reaction of finite speed, where  $\text{He}$  is the Henry's law constant:

$$k_G \text{He} \ll k_L \text{Ha} \quad (36)$$

Suitable reactions are those of  $\text{SO}_2$ ,  $\text{Cl}_2$ , or  $\text{I}_2$  with  $\text{NaOH}$ ,  $\text{SO}_2$  with  $\text{Na}_2\text{CO}_3$  and  $\text{NH}_3$  or triethylamine ( $\text{Et}_3\text{N}$ ) with  $\text{H}_2\text{SO}_4$ .<sup>13</sup> With these systems, the partial pressure of the solute at the interface is negligible. Applying these conditions to a packed column, Eq. 6 leads to an expression for  $k_G$  that is conveniently independent of thermochemical properties:

$$k_G = \frac{G}{\text{Ha}_e} \ln \left( \frac{y_{\text{in}}}{y_{\text{out}}} \right) \quad (37)$$

Table 8 lists the articles in which the method of chemical absorption has been used. Either an acidic solute, such as  $\text{H}_2\text{S}$ ,  $\text{SO}_2$ , or  $\text{CO}_2$ , is absorbed into a basic solution ( $\text{NH}_3$  for  $\text{H}_2\text{S}$  and  $\text{NaOH}$  for  $\text{SO}_2$  and  $\text{CO}_2$ ), or a basic solute, such as  $\text{NH}_3$  is absorbed into an acid, typically  $\text{H}_2\text{SO}_4$ . In recent years, the absorption of  $\text{SO}_2$  into  $\text{NaOH}$  has become the most popular option. The carrier gas has almost always been air except in the work of Vidwans and Sharma,<sup>28</sup> where several freons were used as well, to study the effect of gas phase diffusivity.

The majority of the methods use instantaneous or very fast reactions. A specific alternative is described by Laurent et al.<sup>13</sup> and used by Alix and Raynal.<sup>52</sup> In this case, a fast reaction is used ( $\text{CO}_2 + \text{NaOH}$ ), which satisfies the following conditions:  $\text{Ha} \ll E_{\text{inf}}$  and  $\text{Ha} > 5$ . These are conditions close to those presented in the section "Determination of the Effective Interfacial Area—Chemical absorption—Fast reactions—Methodology" for the determination of  $a_e$  by a chemical method where the liquid-side resistance is independent of  $k_L$  and varies only with  $a_e$ . The difference in this case is that the gas-side resistance is not negligible because of a high  $\text{NaOH}$

**Table 8. Main Characteristics of Methods Using Chemical Absorption to Determine  $k_G$** 

Source	Packing	Gas	Liquid
Fellinger <sup>85</sup>	Berl saddles	NH <sub>3</sub> in air	H <sub>2</sub> SO <sub>4</sub> (aq)
Johnstone and Singh <sup>117</sup>	Grids, plates, wire helices, Raschig rings, spiral rings	NH <sub>3</sub> in air SO <sub>2</sub> in air	Acetic acid (aq) NaOH (aq)
Van Krevelen et al. <sup>118</sup>	Glass rings	H <sub>2</sub> S in air	NH <sub>3</sub> (aq) (NH <sub>4</sub> ) <sub>2</sub> SO <sub>4</sub> (aq)
Vidwans and Sharma <sup>28</sup>	Raschig rings, Intalox saddles	NH <sub>3</sub> in air NH <sub>3</sub> in air or freons Et <sub>3</sub> N in air or freons SO <sub>2</sub> in air or freons Cl <sub>2</sub> in air or freons	H <sub>2</sub> SO <sub>4</sub> (aq) Acetic acid (aq) NaOH (aq)
Weiland et al. <sup>40</sup>	Goodloe, Montz A2	SO <sub>2</sub> in air	NaOH (aq)
Nakov and Kolev <sup>119</sup>	Turbo-Pack	NH <sub>3</sub> in air	H <sub>2</sub> SO <sub>4</sub> (aq)
Moucha et al. <sup>120</sup>	Modified Intalox saddles	SO <sub>2</sub> in air	NaOH (aq)
Hoffmann et al. <sup>8</sup>	Pall rings	SO <sub>2</sub> in air	NaOH (aq)
Kim and Deshusses <sup>121</sup>	Lava rocks, porous ceramic beads and Raschig rings, Pall rings, polyurethane foam	CO <sub>2</sub> in air	NaOH (aq)
Alix and Raynal <sup>52</sup>	IMTP50	CO <sub>2</sub> in air or of the air	NaOH (aq)
Wang et al. <sup>55,56</sup>	Mellapak 2X, 250.X, 250.Y, Flexipac, Raschig Super-Pak, Raschig Super-Ring, Pall rings, GT-Pak 350Y, 350Z	SO <sub>2</sub> in air	NaOH (aq)
Rejl et al. <sup>57</sup>	Super-Pak 250.Y	SO <sub>2</sub> in air	NaOH (aq)
Kunze et al. <sup>10</sup>	Pall rings, Mellapak 250.Y	NH <sub>3</sub> in air	H <sub>2</sub> SO <sub>4</sub> (aq)

concentration that leads to a CO<sub>2</sub> concentration gradient in the gas film by increased reaction rate. In this situation, a Danckwerts' plot method can be applied using the expression for the ratio of the partial pressure of the solute ( $p$ ) and the volumetric rate of absorption ( $\Phi$ ). For a pseudo-first order reaction, this expression is:

$$\frac{p}{\Phi} = \frac{1}{k_G a_e} + \frac{He}{\sqrt{kDB^0} a_e} \quad (38)$$

The left-hand side can be plotted as a function of  $He/\sqrt{kDB^0}$ . The interfacial area is determined from the slope,  $k_G a_e$  from the intercept. Although this method can be used to determine  $k_G$ , due to potentially large uncertainties in the determination of the intercept, it is better suited for taking into account gas-side resistance during the determination of  $a_e$ . Moreover, it is more labor intensive, as repeated experiments with different values of  $k$  or  $B^0$  must be performed.

As regards liquid-side resistance, most authors have neglected it without verification but not all. Johnstone and Singh<sup>117</sup> verified this assumption by plotting  $1/K_G a_e$  as a function of  $1/u_G^{0.8}$ , where  $u_G$  is the superficial velocity of the gas. A straight line fitted to the measurement points was found to intercept the origin when extrapolated. At the origin  $1/u_G^{0.8} = 0$ , and  $1/K_G a_e$  equals the liquid-side resistance according to Eq. 30. Thus, the fitted line passing through the origin is hinting to an inexistent liquid-side resistance. Vidwans and Sharma<sup>28</sup> studied the effect of  $L$  on both  $k_G a_e$  and  $k_G$  and observed that the variation of  $k_G a_e$  with  $L$  was entirely due to that of  $a_e$ , meaning that  $k_G$  was really the true gas-side mass-transfer coefficient. The system CO<sub>2</sub>-NaOH<sup>52</sup> stands apart from the rest, as the reaction belongs to the fast reaction regime, and the liquid-side resistance can be accounted for by the kinetics of the reaction system alone, but it requires more work. On the other hand, Kim and Deshusses<sup>121</sup> treated this reaction as an instantaneous one, as they found no influence of the NaOH concentration on the absorption rate above a pH of 13.

Although only applied by Kunze et al.<sup>10</sup> by recirculating the gas phase, Hoffmann et al.<sup>8</sup> recommended to saturate the gas stream with water prior to absorption in order to avoid

temperature effects and multicomponent mass transfer due to the evaporation of water. The magnitude of the errors introduced was not discussed. The most important effect of the cooling down of air is possibly the change in gas-phase diffusivity. Sharma and Danckwerts,<sup>12</sup> among others, advised to always perform the calculation of  $k_G a_e$  based on the measured gas phase concentrations, more precise than those of liquid phase.

Sherwood and Holloway<sup>88</sup> recommend the method of chemical absorption instead of vaporization of a pure liquid due to the potential experimental difficulties such as the necessity of short beds and careful control of liquid temperature. However, the packed bed height may be limited in this case as well, because the rapid consumption of the solute can lead to absolute residual values in the gas phase so small as to be within the uncertainty limits of practical analytical devices.

The main advantage of the method of chemical absorption is the near complete elimination of the liquid-side resistance, if the reaction fulfills the necessary criteria, so that the reaction takes place at the gas-liquid interface. Disadvantages are that chemical analysis is required, and that the packed bed height might be limited due to the depletion of the solute in the gas phase.

### Conclusion

The methods used for the determination of  $k_G a_e$  belong to one of the three following groups: vaporization of a pure liquid, physical absorption, or chemical absorption. Each of these aims to eliminate the liquid-side resistance or at least to reduce it to a value that can be safely neglected. If a pure liquid is vaporized, this is naturally accomplished. By physical absorption of a very soluble compound, the liquid-side resistance can be greatly reduced if appropriate  $G/L$  ratios are used. However, the liquid-side resistance, no matter how low, always exists, and it is suggested to check its magnitude either by a correlation or by using literature values. If the liquid-side resistance is not negligible, it is also possible to obtain  $k_G a_e$  by subtracting  $k_L a_e$  from the overall mass-transfer coefficient, or by separating the two resistances based on certain

assumptions. However, these approaches seem to be prone to include additional errors in  $k_G a_e$ . By chemical absorption, an instantaneous or very fast reaction ensures that the solute is consumed at the gas-liquid interface, eliminating the resistance from the liquid film. It is then necessary to check that the conditions set the system in the appropriate reaction regime.

From a practical point of view, each group of methods suffers from some type of disadvantage. In general, quick saturation or depletion of the gas phase limits the height of the packed bed that can be used due to uncertainties in analytical system for measuring relative concentration changes. By vaporization, the saturation value also contains experimental error, as it is calculated from measured liquid temperatures. Physical and chemical absorption require handling chemicals, and performing chemical analyses, yet another source of uncertainties, while the measurement of temperatures and humidities is sufficient for the vaporization of water.

Of these various methods, using chemical absorption in the instantaneous regime is recommended first as the results are independent of thermochemical properties, with choice reactions systems being air diluted  $\text{SO}_2$  or  $\text{NH}_3$  into  $\text{NaOH}$  or  $\text{H}_2\text{SO}_4$  solutions respectively. If the nature of the chemicals is an issue then physical desorption is an option if  $k_L$  is known or is negligible, otherwise evaporation methods should be used.

### Determination of the Liquid-Side Mass-Transfer Coefficient

As with gas-side mass-transfer coefficients, the methods described in the literature provide column averaged volumetric liquid-side mass-transfer coefficients  $k_L a_e$ . Local values cannot be determined directly as measurement techniques for local concentrations in the gas or liquid film are not currently available. It is generally assumed that the gas-side mass transfer resistance is negligible, and thus  $K_L a_e = k_L a_e$ . If the gas phase is pure, this assumption is entirely valid. Otherwise, gas-side resistance is present to a degree that depends on the chemical system as well as on the flow conditions. Once  $k_L a_e$  has been measured, the value of  $k_L$  can be calculated by dividing by  $a_e$  for the type of mass transfer process used. To determine the liquid-side mass-transfer coefficient, the following groups of methods can be applied:

- physical absorption,
- desorption,
- chemical absorption.

In the next sections, the methods found in the literature are presented, and the advantages and drawbacks of each group of methods are discussed.

#### Physical absorption

Methods using physical absorption have been used extensively since the 1930s. Table 9 presents the literature using this principle, along with the chemical systems and basis of the determination of  $k_L a_e$ .

The majority of the methods use a solute gas component of very low solubility such that the mass transfer resistance lies predominantly within the liquid film while the gas-side resistance is negligible. However, low solubilities can lead to quick saturation of the liquid phase, a situation that induces large experimental uncertainties, and that can occur especially if the gas is purely the solute.<sup>26</sup> The dominance of liquid-side resistance will be favored at low  $L/G$  values.

When gases with high solubility are used then the gas-side resistance is not negligible, and should be obtained either from another means, or by simultaneous evaluation with  $k_L a_e$ . In the first case the liquid-side resistance, and thus  $k_L a_e$  can be obtained by subtracting the gas-side resistance  $1/k_G a_e$  from the measured overall resistance. Either  $k_G a_e$  is measured by an appropriate method at the same conditions (e.g., Hoffmann et al.<sup>8</sup>) or it can be estimated from a correlation (e.g., Scheibel and Othmer<sup>104</sup>) This procedure, however, is only correct if  $a_e$  is the same for the methods by which  $k_G a_e$  and  $k_L a_e$  were measured: for example, if  $k_G a_e$  and  $a_e$  were measured by chemical absorption while  $k_L a_e$  was determined by physical absorption, then an error is introduced into  $k_L$ .<sup>9</sup> This is the case with the results of Hoffmann et al.<sup>8</sup> who implicitly assume the equality of areas. This problem can be overcome by using the correct effective areas for each measurement:

$$\frac{1}{k_L} = \frac{(a_e)_L}{(K_L a_e)_L} - \frac{(a_e)_G}{m(k_G a_e)_G} \quad (39)$$

A disadvantage of measuring or estimating  $k_G a_e$  separately is that its error is propagated to  $k_L a_e$ . The higher the gas-side resistance, the more important this effect. In the second case, the simultaneous determination of  $k_G a_e$  and  $k_L a_e$  can be obtained based on assumptions on their dependencies to gas and liquid flow rates (see the section “Determination of the Gas-Side Mass-Transfer Coefficient—Physical absorption”). It is generally assumed that  $k_L a_e$  is independent of  $G$  (Assumption 1, Eq. 30), and, except for Whitney and Vivian,<sup>99</sup> that  $k_G a_e$  is proportional to  $G^{0.8}$  (Eq. 31). Although this method can be used to determine  $k_L a_e$ , it was used in the literature sources with the primary aim of obtaining  $k_G a_e$  in measurements where the majority of the mass transfer resistance is located in the gas film with a secondary but non-negligible contribution of the liquid film resistance. This is not a recommended condition for  $k_L a_e$  as the aim of this procedure is primarily the determination of  $k_G a_e$ , and although  $k_L a_e$  is also obtained, it is likely to contain the greater part of measurement errors.

The most commonly used system has been the absorption of  $\text{CO}_2$  in water. The  $\text{CO}_2$  has often been pure, but also mixed into carrier gases such as air or  $\text{N}_2$  at concentration between 3 and 15 mol%, or even up to 48 mol% in the case of Payne and Dodge.<sup>122</sup> Laso et al.<sup>3</sup> pointed out potential drawbacks of using  $\text{CO}_2$  relative to other poorly soluble gases. First, the solubility of  $\text{CO}_2$  is greater than that of  $\text{O}_2$ ,  $\text{H}_2$ , or  $\text{N}_2$ . Second, the absorption of  $\text{CO}_2$  into water involves chemical reactions with the formation of carbonic acid, and although these should not normally influence the mass transfer rate, the presence of cations in non-demineralized water can have an effect. Third, if solid precipitations are formed with the cations, even in very low amounts, they may modify the wettability of the packing by adhering to its surface. Laso et al.<sup>3</sup> performed desorption experiments, but their remarks are equally valid for absorption.

Some authors have used various aqueous solutions to study the effect of liquid properties, such as viscosity and surface tension. Organic solvents, most frequently methanol, were also applied with the same purpose. Van Krevelen et al.,<sup>118</sup> Linek et al.,<sup>39</sup> Moucha et al.,<sup>120</sup> Kim and Deshusses<sup>121</sup>, and San-Valero et al.<sup>116</sup> used the absorption of  $\text{O}_2$  into water. Onda et al.,<sup>131</sup> in addition to  $\text{CO}_2$ , performed measurements of  $\text{H}_2$  absorption into water to determine the dependency of  $k_L a_e$  to  $\text{Sc}_L$ .

**Table 9. Main Characteristics of the Methods Using Physical Absorption to Determine  $k_L$**

Source	Packing	Gas	Liquid	Principle
Payne and Dodge <sup>122</sup>	Rings	CO <sub>2</sub> in air	Water	Gas-side resistance neglected
Data of Allen <sup>123</sup> reported by Sherwood and Holloway <sup>98</sup>	Raschig rings	CO <sub>2</sub>	Water	Gas-side resistance neglected
Othmer and Scheibel <sup>102</sup>	Raschig rings	Acetone in air	Water	Assumption 1 + 2
White and Othmer <sup>103</sup>	Stedman triangular pyramid	Acetone in air	Water	Assumption 1 + 2
Scheibel and Othmer <sup>104</sup>	Raschig rings	Acetone in air Butanone in air Methyl isobutyl ketone in air 2-Heptanone in air	Water	Assumption 1 + 2 $k_G$ subtracted from $K_L$
Van Krevelen and Hoftijzer <sup>124</sup>	Rings	O <sub>2</sub>	Aqueous suspension of Prussian white	Gas-side resistance neglected
Landau et al. <sup>108</sup>	Raschig rings	UF <sub>6</sub> in N <sub>2</sub>	Heavy oil	Assumption 1
Van Krevelen et al. <sup>118</sup>	Rings	NH <sub>3</sub>	Water	Assumption 1 + 2
Hutchings et al. <sup>109</sup>	Raschig rings	Acetone in air	Water	Assumption 1 + 2
Whitney and Vivian <sup>99</sup>	Raschig rings	SO <sub>2</sub> (saturated with water)	Water	Assumption 1
Koch et al. <sup>125</sup>	Raschig rings	CO <sub>2</sub> in air	Water	Gas-side resistance neglected
Hikita et al. <sup>126</sup>	Raschig rings, Berl saddles (stacked/dumped, with and without paraffin coating)	Pure CO <sub>2</sub>	Water	No gas-side resistance
Ueyama et al. <sup>127</sup>	Rings	Pure CO <sub>2</sub>	Water	No gas-side resistance
Fujita and Hayakawa <sup>128</sup>	Raschig rings, Berl saddles	Pure CO <sub>2</sub>	Water	No gas-side resistance
Yoshida and Koyanagi <sup>73</sup>	Raschig rings, Berl saddles, spheres	Pure CO <sub>2</sub> (saturated with absorbent)	Water Methanol	No gas-side resistance
Onda et al. <sup>129</sup>	Raschig rings	Pure CO <sub>2</sub>	Water	No gas-side resistance
Hikita et al. <sup>130</sup>	Raschig rings	Pure CO <sub>2</sub>	Water	No gas-side resistance
Onda et al. <sup>131</sup>	Raschig rings	Pure CO <sub>2</sub>	Water	No gas-side resistance
Onda and Sada <sup>132</sup>	Raschig rings	Pure H <sub>2</sub> (saturated with absorbent) Pure CO <sub>2</sub>	Water Methanol Ethanol CCl <sub>4</sub> Benzene Decaline	No gas-side resistance
Hikita et al. <sup>74</sup>	Raschig rings, Berl saddles	Pure CO <sub>2</sub>	Water Sugar (aq) Methanol (aq) Methanol	No gas-side resistance
Onda et al. <sup>133</sup>	Spheres	Pure CO <sub>2</sub>	Water	No gas-side resistance
De Waal and Beek <sup>134</sup>	Raschig rings	CO <sub>2</sub> in air (saturated with water)	Water	Gas-side resistance neglected
Onda et al. <sup>96</sup>	Raschig rings, Berl saddles, spheres, rods	CO <sub>2</sub>	Water (+ surfactant) Methanol CCl <sub>4</sub>	No gas-side resistance No gas-side resistance
Merchuk et al. <sup>135</sup>	Raschig rings	Pure CO <sub>2</sub>	Water	No gas-side resistance
Sahay and Sharma <sup>32</sup>	Raschig rings, Pall rings, Intalox saddles	Pure CO <sub>2</sub>	Water	No gas-side resistance
Joosten and Danckwerts <sup>22</sup>	Raschig rings, Intalox saddles	Pure CO <sub>2</sub>	NaNO <sub>3</sub> + sugar (aq)	No gas-side resistance
Maćkowiak <sup>136</sup>	Raschig rings, Bialecki rings, I-13 rings	CO <sub>2</sub> in air	Water	Gas-side resistance neglected
Merchuk <sup>36</sup>	Raschig rings, flat rings, spirals, saddles	CO <sub>2</sub> in air or in pure form	Water	Gas-side resistance neglected or no gas-side resistance
Mangers and Ponter <sup>137,138</sup>	Raschig rings	Pure CO <sub>2</sub> (saturated with water)	Water Glycerol (aq)	No gas-side resistance
Billet and Maćkowiak <sup>114,139</sup>	Pall rings, NSW rings, Hiflow rings, Hacketts, Impulse type 50	CO <sub>2</sub> in air	Water	Gas-side resistance neglected
Linek et al. <sup>39</sup>	Pall rings	O <sub>2</sub> of the air	Water	Gas-side resistance neglected
Maćkowiak <sup>115</sup>	Montz B1, C1, Gempak 2A	CO <sub>2</sub> in air	Water	Gas-side resistance neglected
Benadda et al. <sup>24</sup>	Berl saddles	CO <sub>2</sub> in N <sub>2</sub>	Water	Gas-side resistance neglected
Moucha et al. <sup>120</sup>	Modified Intalox saddles	O <sub>2</sub> of the air	Water	Gas-side resistance neglected
Hoffmann et al. <sup>8</sup>	Pall rings	NH <sub>3</sub> in air (saturated with water)	Water	$k_G$ subtracted from $K_G$
Kim and Deshusses <sup>121</sup>	Lava rocks, porous ceramic beads and Raschig rings, Pall rings, polyurethane foam	O <sub>2</sub> of the air	Water	Gas-side resistance neglected
San-Valero et al. <sup>116</sup>	Flexiring, Refilltech, PAS Winded Media	O <sub>2</sub> of the air	Water	Gas-side resistance neglected

**Table 10. Main Characteristics of the Methods Using Desorption to Determine  $k_L$**

Source	Packing	Gas	Liquid
Sherwood and Holloway <sup>98</sup>	Raschig rings, Berl saddles, tiles	Air	CO <sub>2</sub> in water O <sub>2</sub> in water H <sub>2</sub> in water
Molstad et al. <sup>107,140</sup>	Raschig rings, Berl saddles, spiral rings, partition rings, drip-point grids, wood grids	Air	O <sub>2</sub> in water
Jones <sup>141</sup>	Raschig rings	Air	CO <sub>2</sub> in water
Vivian and Whitney <sup>142</sup>	Raschig rings	Air	O <sub>2</sub> in water
Deed et al. <sup>143</sup>	Raschig rings	Air	CO <sub>2</sub> in water O <sub>2</sub> in water
Landau et al. <sup>108</sup>	Raschig rings	N <sub>2</sub>	UF <sub>6</sub> in heavy oil
Whitney and Vivian <sup>99</sup>	Raschig rings	Air	O <sub>2</sub> in water
Vivian and King <sup>144</sup>	Raschig rings	Air (saturated with water)	CO <sub>2</sub> in water O <sub>2</sub> in water H <sub>2</sub> in water Propene in water
Linek et al. <sup>39</sup>	Pall rings	N <sub>2</sub> (saturated with water)	O <sub>2</sub> in water
Henriques de Brito et al. <sup>145</sup>	Mellapak 250.Y, 500.Y	Air	O <sub>2</sub> in water
Kolev and Nakov <sup>146</sup>	Turbo-Pack	Air	CO <sub>2</sub> in water
Laso et al. <sup>3</sup>	Mellapak 125.Y, 250.Y, 500.Y	Air (saturated with water)	O <sub>2</sub> in water
Brunazzi and Paglianti <sup>147</sup>	Mellapak 250.Y, Sulzer BX	Air	CO <sub>2</sub> in water
Murrieta et al. <sup>97</sup>	Flexipac-2, Intalox 1T, Intalox 2T, Sulzer BX, Pall rings	Air	O <sub>2</sub> in water
Valenz et al. <sup>4</sup>	Mellapak 250.Y, 350.Y, 452.Y, 500.Y	N <sub>2</sub> (saturated with water)	O <sub>2</sub> in water
Wang et al. <sup>5,55,56</sup>	Mellapak 2X, 250.X, 250.Y, GT-Pak 350Y, 350Z, 500Y, A 350Y, B 350X, Raschig Hybrid 200X, 250Y, Flexipac, Raschig Super-Pak, Raschig Super-Ring, Pall rings	Air	Toluene in water
Rejl et al. <sup>57</sup>	Super-Pak 250.Y	N <sub>2</sub> (saturated with water)	O <sub>2</sub> in water
Kunze et al. <sup>10</sup>	Pall rings, Mellapak 250.Y	Air	CO <sub>2</sub> in water

Systems where  $k_L a_e$  was determined by subtracting out the gas-side resistance from  $K_G a_e$  or  $K_L a_e$  include the absorption of NH<sub>3</sub> (0.2–1.29 mol%) into water,<sup>8</sup> and the absorption of ketones with longer carbon chain (0.07–2.59 mol%) into water,<sup>104</sup> where  $k_G a_e$  was too low to be measured simultaneously using Assumptions 1 and 2.

Cases where  $k_G a_e$  and  $k_L a_e$ , were determined simultaneously involved the absorption of NH<sub>3</sub>, SO<sub>2</sub> or ketones into water. Landau et al.<sup>108</sup> also performed the absorption of UF<sub>6</sub> into a heavy oil. The solutes were mixed to either air or N<sub>2</sub> in the concentration range of 0.12–18 mol%.

Several authors<sup>8,39,73,99,131,134,137,138</sup> saturated the gas phase with the absorbent before the absorption column in order to avoid the evaporation of the liquid. The effects of evaporation were discussed in the section “Determination of the Gas-Side Mass-Transfer Coefficient—Physical absorption.”

In summary, the determination of  $k_L a_e$  by physical absorption of a poorly soluble gas has been widely applied in the literature. The gas-side resistance is completely eliminated if the gas phase is pure, but due to the low solubility of the gas, it is customarily neglected even if the solute is mixed to a carrier gas. The system CO<sub>2</sub>—water is applied in the majority of the cases: it can be easily handled and the gas phase concentration can be conveniently measured by an infrared gas analyzer. If pure CO<sub>2</sub> is used, care must be taken to avoid the saturation of the liquid phase. If the solubility of the gas is not low enough to neglect gas-side resistance,  $k_G a_e$  can be measured separately or calculated by a correlation, however, the obtained  $k_L a_e$  values will be affected by the eventual uncertainties of  $k_G a_e$ .

### Desorption

The desorption of a poorly soluble gas can also be used to determine  $k_L a_e$ . As with physical absorption, the gas-side resistance can be neglected if the solubility is low enough. If the partial pressure of the solute in the gas phase is negligible then for a packed column, Eq. 9 leads to an expression for  $k_L$  that is conveniently independent of thermochemical properties:

$$k_L = \frac{L}{Ha_e} \ln \left( \frac{x_{in}}{x_{out}} \right) \quad (40)$$

Desorption is more convenient to implement<sup>4</sup> with better accuracy than physical absorption.<sup>98</sup> With a low solubility solute the fractional gas-side concentration gradient along the column becomes small within only a short height. This leads to uncertainties in evaluating the desorption flux from gas phase measurements for long beds. The liquid phase solute concentration is therefore the preferred measurement. The maximum bed height is then only constrained by detection limit of the analytical method. Landau et al.<sup>108</sup> did not use a poorly soluble gas, but applied their method presented in the section “Determination of the Liquid-Side Mass-Transfer Coefficient—Physical absorption” to also simultaneously determine  $k_G a_e$  and  $k_L a_e$  by desorption. Table 10 lists the articles using desorption.

The solutes that have been used are CO<sub>2</sub> and O<sub>2</sub> in the majority of the literature sources, owing to their ease of use and analysis. H<sub>2</sub><sup>98</sup> and organic compounds with limited solubilities in water (propene and toluene) have also been used.

**Table 11. Main Characteristics of the Methods Using Chemical Absorption to Determine  $k_L$** 

Source	Packing	Gas	Liquid	Principle
Van Krevelen and Hoftijzer <sup>124</sup>	Rings, spheres	CO <sub>2</sub>	Caustic solution	Instantaneous reaction
Van Krevelen et al. <sup>118</sup>	Rings	NH <sub>3</sub> in air	H <sub>2</sub> SO <sub>4</sub> (aq)	Instantaneous reaction
		H <sub>2</sub> S in air	NaOH (aq)	
Danckwerts and Gillham <sup>60</sup>	Raschig rings	Pure CO <sub>2</sub> (saturated with water vapor)	K <sub>2</sub> CO <sub>3</sub> + KHCO <sub>3</sub> + NaOCl (aq)	Danckwerts' plot and analogy with a stirred cell
			NaOH + Na <sub>2</sub> SO <sub>4</sub> (aq)	Analogy with a stirred cell
De Waal and Beek <sup>134</sup>	Raschig rings	O <sub>2</sub> of the air	Na <sub>2</sub> SO <sub>3</sub> + Co <sup>2+</sup> (aq)	Danckwerts' plot
Jhaveri and Sharma <sup>29</sup>	Raschig rings	O <sub>2</sub> of the air	CuCl + HCl (aq)	Danckwerts' plot
Onda et al. <sup>31</sup>	Raschig rings	O <sub>2</sub> of the air, in air, or in pure form	Na <sub>2</sub> SO <sub>3</sub> + CoSO <sub>4</sub>	Danckwerts' plot
Joosten and Danckwerts <sup>22</sup>	Raschig rings, Intalox saddles	Pure CO <sub>2</sub>	KHCO <sub>3</sub> + K <sub>2</sub> CO <sub>3</sub> + KAsO <sub>2</sub> (aq)	Danckwerts' plot
			K <sub>2</sub> HPO <sub>4</sub> + KH <sub>2</sub> PO <sub>4</sub> (aq)	Slow reaction
			NaOH + NaNO <sub>3</sub> + sugar (aq)	Instantaneous reaction
Rizzuti et al. <sup>37,61</sup> , Rizzuti and Brucato <sup>62</sup>	Raschig rings	Pure CO <sub>2</sub>	K <sub>2</sub> CO <sub>3</sub> + KHCO <sub>3</sub> + KAsO <sub>2</sub> - sugar (aq)	Danckwerts' plot
Weiland et al. <sup>40</sup>	Montz A2, Goodloe	CO <sub>2</sub> in air	Na <sub>2</sub> CO <sub>3</sub> + NaHCO <sub>3</sub> (aq)	Slow reaction
Benadda et al. <sup>42</sup>	Raschig rings	CO <sub>2</sub> in air	Na <sub>2</sub> CO <sub>3</sub> + NaHCO <sub>3</sub> + NaOCl (aq)	Danckwerts' plot
Roesler et al. <sup>148</sup>	Mellapak 250.X, 250.Y, IFPACC™ 2X	CO <sub>2</sub> in air	MDEA + CO <sub>2</sub> (aq)	Slow reaction

Laso et al.<sup>3</sup> have warned that the solubility of CO<sub>2</sub> is rather high compared to that of O<sub>2</sub>, for example, and that the cations present in water (unless deionized) might affect the results. The liquid phase has been water in all sources, and the gas phase air or, in one case N<sub>2</sub>.<sup>4</sup> Vivian and King,<sup>144</sup> Linek et al.,<sup>39</sup> Laso et al.,<sup>3</sup> Valenz et al.,<sup>4</sup> and Rejl et al.<sup>57</sup> humidified the gas phase before the desorption column to minimize liquid interfacial temperature gradients from evaporation. Kunze et al.<sup>10</sup> achieved saturation of the gas phase by recirculating it.

The saturation of the water with the solute was realized in different ways. Several authors<sup>97,99,146</sup> introduced the gas into the water stream before the column from a gas cylinder, some<sup>3,39,147</sup> saturated the water in a tank before the experiments, while others used an absorption column.<sup>143,144</sup> Wang et al.<sup>55</sup> simply mixed toluene and water in a tank at the start of the experiment since their solute is a liquid at room temperature, and then continuously added a toluene make-up into the tank, because their liquid phase was recirculated.

In summary, the desorption of a poorly soluble gas, typically CO<sub>2</sub> or O<sub>2</sub> into water, is a convenient and popular method to determine  $k_L a_c$ . The use of O<sub>2</sub> is likely to yield more precise results. The gas-side resistance is never completely eliminated, but the low solubility makes it negligible. Chemical analysis, usually that of the liquid phase, is necessary, but for the gases mentioned above, the analysis methods are well established.

### Chemical absorption

The liquid-side mass-transfer coefficient can also be determined by methods using chemical absorption. The reactions applied belong to three different reaction regimes: they can be instantaneous (or very fast), of intermediate speed, or slow. The resistance of the gas phase has to be negligible, which is often the case with the systems and conditions used. An overview of these methods is given by Sharma and Danckwerts<sup>12</sup> and Laurent et al.<sup>13</sup> Danckwerts and Gillham<sup>60</sup> used a particular approach using the analogy of the packed column to a stirred cell. The methods found in the literature are listed in Table 11, where the principle of the determination of  $k_L a_c$  is also given.

*Instantaneous or Very Fast Reactions.* A reaction can be considered instantaneous if:

$$Ha \gg E_{inf} \quad (41)$$

Sharma and Danckwerts<sup>12</sup> give this condition:

$$Ha > 10E_{inf} \quad (42)$$

In practice, the constraint can be relaxed to  $E_{inf} > 4$ .<sup>13</sup> This is the same reaction regime as the one used for the determination of  $k_G a_c$ , but here the condition on  $k_G$  is inverted:

$$k_G p \gg k_L B^0 \quad (43)$$

This means that the gas-side resistance is negligible, and the reaction does not take place on the gas-liquid interface.

When the following additional criterion:

$$\frac{D_B B^0}{D_A v A^*} \gg 1 \quad (44)$$

is also met, meaning that the liquid phase reagent is in great excess compared to the equilibrium concentration of the solute in the liquid phase without reaction, then the enhancement factor becomes:

$$E \approx E_{inf} = \frac{D_B B^0}{D_A v A^*} \quad (45)$$

This ensures that the solute concentration is virtually zero in the bulk liquid ( $A^0 = 0$ ). By substitution, the volumetric mass transfer rate becomes independent of the concentrations  $A^0$  and  $A^*$ :

$$\Phi = E k_L a_c (A^* - A^0) = \frac{D_B B^0}{D_A v} k_L a_c \quad (46)$$

and  $k_L a$  can be calculated merely by measuring  $B^0$ . An advantage of this method is that it is not necessary to know the solubility of  $A$ . In essence, what is happening is that the limiting factor is the diffusion of the reagent to the reaction zone near the interface within the liquid film and not the reaction rate, therefore the flux is controlled by only physical terms.

Reactions that can be used (Table 11) include the absorption of  $\text{NH}_3$  into sulfuric acid, of  $\text{SO}_2$ ,  $\text{Cl}_2$ , or  $\text{HCl}$  into alkalis, of  $\text{H}_2\text{S}$  or  $\text{HCl}$  in solutions of amines. Under certain conditions, the absorption of  $\text{O}_2$  from air into dithionite solution, or that of pure  $\text{CO}_2$  into amine solutions can also be appropriate.<sup>12</sup> Van Krevelen and Hofstijzer<sup>124</sup> and Joosten and Danckwerts<sup>22</sup> used the absorption of  $\text{CO}_2$  into caustic solutions.

*Danckwerts' Plot (Intermediate Reaction Regime).* If the reaction is in the intermediate reaction regime, ( $\text{Ha} \ll E_{\text{inf}}$  and  $E < 9$  according to Sharma and Danckwerts<sup>12</sup>) the Danckwerts' plot can be used to simultaneously determine  $k_L$  and  $a_e$ . The method was described in detail in the section "Determination of the Effective Interfacial Area—Chemical absorption—Danckwerts' plot (intermediate reaction regime)." The uncertainty of  $k_L$  is higher than that of  $a_e$ , as it is determined from the intercept of the plot  $\Phi^2 - kB^0$ , while  $a_e$  is calculated from the slope. If the gas-side resistance is not negligible, it can also be taken into account.

Reaction systems used have been the absorption of  $\text{CO}_2$  into sodium or potassium bicarbonate buffer solutions, with either  $\text{NaOCl}$  or  $\text{KAsO}_2$  as catalyst (Table 11). The Danckwerts' plot was created by varying the concentration of the catalyst. Under certain conditions, the reaction of  $\text{O}_2$  and  $\text{CuCl}$  can belong to this regime.<sup>29</sup> Some authors absorbed  $\text{O}_2$  into solutions of sodium sulfite with  $\text{Co}^{2+}$  ions as catalyst.

When the solute was  $\text{CO}_2$ , most authors used it in pure form, except Benadda et al.<sup>42</sup> where the  $\text{CO}_2$  concentration was 10% in air. The authors estimated the gas-side resistance to be negligible. The absorption of  $\text{O}_2$  was performed by using air, except for Onda et al.<sup>31</sup> who ran experiments over the entire concentration range from air to pure  $\text{O}_2$ . The gas phase was humidified by air before the absorption in some cases<sup>60,134</sup> in order to reduce evaporation and avoid cooling of the liquid phase.

*Slow Reactions.* In the slow reaction regime, the rate of solute reaction in the liquid film is small to the extent that concentration of the solute can be considered constant in the film, and thus  $E \approx 1$ . The criterion for this condition is that:

$$\text{Ha} < 1 \quad (47)$$

as specified by Laurent et al.,<sup>13</sup> or:

$$\text{Ha}^2 \ll 1 \quad (48)$$

according to Sharma and Danckwerts.<sup>12</sup>

The reaction must simultaneously be fast enough to keep the solute concentration negligibly small in the bulk liquid. The following inequality must then be satisfied:

$$k_L a_e \ll l k B^0 \quad (49)$$

where  $l$  is the volume of liquid phase per unit volume of packing. When these conditions are met, the volumetric mass transfer rate is equal to that of physical absorption:

$$\Phi = k_L a_e A^* \quad (50)$$

therefore,  $k_L a_e$  can be calculated by measuring the absorption rate, and by knowledge of  $A^*$ . If the concentration of  $A$  in the bulk gas is approximately constant, then  $A^*$  is also constant, and can be easily calculated; otherwise, the variation of  $A$  in the column must be estimated. Advantageously, neither the kinetics, nor  $B^0$  for that matter need to be known with great precision as they do not appear in the mass transfer rate expression. Note that gas-side resistance was neglected here.

If the reaction is not fast enough to consume all the solute in the bulk liquid, the following approach can be used. The measured reactive volumetric mass-transfer coefficient  $k_{L,R}$  is:

$$\frac{1}{k_{L,R} a_e} = \frac{1}{k_L a_e} + \frac{1}{l k B^0} \quad (51)$$

By varying either  $k$  (through catalyst concentration), or  $B^0$ , and plotting  $1/k_{L,R} a_e$  against  $k B^0$  as a straight line,  $k_L a_e$  can be obtained from the intercept.

According to Sharma and Danckwerts,<sup>12</sup> suitable chemical systems are the absorption of  $\text{CO}_2$  into carbonate-bicarbonate buffer solution without catalyst, or that of  $\text{O}_2$  into dilute acid solutions of  $\text{CuCl}$ , or into  $\text{Na}_2\text{SO}_3$  solution using  $\text{CoSO}_4$  or  $\text{CuSO}_4$  as catalyst. For packed columns, the absorption of  $\text{CO}_2$  into bicarbonate and phosphate buffer solutions were used (Table 11). Recently, Roesler et al.<sup>148</sup> used a system based on the absorption of low partial pressures of  $\text{CO}_2$  (1.5 kPa or less) into a partially loaded solution of dilute methyl diethanolamine (MDEA) solutions (3% wt) to determine the  $k_L a$  of various structured packings. These reactants provided an irreversible pseudo-first order reaction system in the slow regime for loadings between 0.1 and 0.2 mol- $\text{CO}_2$ /mol-MDEA. The rather weak absorption fluxes and consequently slow depletion rates of the gas phase solute make this method well suited for columns with  $\text{NTU}_L$  greater than 2 where physical desorption methods may lead to high uncertainties.

*Analogy Between a Packed Column and a Stirred Cell.* This method was used by Danckwerts and Gillham,<sup>60</sup> and is described in the section "Determination of the Effective Interfacial Area—Chemical absorption—Other methods." The main idea is that if the enhancement factors in a stirred cell and in a packed column are equal for the same chemical system and compositions, then the  $k_L$  values are also equal.  $\text{CO}_2$  is absorbed into inert and reactive solutions such as those of bicarbonate buffer and  $\text{NaOH}$  in water. For any stirring speed of the cell, there exists a liquid flow rate of the packed column at which the enhancement factors of both systems are equal. At this point, the  $k_L$  measured in the stirred cell is equal to that of the column. Since the interfacial area of the stirred cell is known, it is possible to measure  $k_L$  instead of  $k_L a_e$ .

*Conclusion on Chemical Absorption Methods.* The chemical absorption methods use a variety of reaction systems, belonging to three reaction regimes, to determine the liquid-side mass-transfer coefficient and usually involving the absorption of  $\text{CO}_2$  and  $\text{O}_2$ . The intermediate regime is the one most frequently applied, whereby the method of the Danckwerts' plot is used, although  $k_L$  is likely to be more uncertain, since it is calculated from the intercept of the plot. Bicarbonate buffer solutions with different catalysts have been applied by several authors. Whatever the regime, the test conditions must be carefully checked to satisfy the required criteria, as their validity may change from run to run and even along the column, depending on the concentration of the reagents.

### Tomography

A novel method proposed by Schug and Arlt<sup>149</sup> aims to determine  $k_L$  by computer tomography using x-rays. The idea is to measure the concentration of the solute directly in the liquid phase, by relating the greyscale values of the pixels (resolution:  $80.52 \mu\text{m} \times 80.52 \mu\text{m}$ ) in the liquid phase to the local solute concentration. The solute must have high molecular weight to absorb x-rays sufficiently, and must be soluble enough to reach sufficient concentrations for identification.

Dichloromethane was identified as a good solute candidate. The authors stated that the liquid film on the packing is thick enough (at least 10 pixels) to enable the application of the method if the viscosity is higher than 2 mPa-s, and they recommend absorption into isopropanol or other alcohols with longer carbon chains. The tests were performed in a 5 cm diameter column filled with 20 cm of an unspecified Mellapak packing. At the time of the completion of this manuscript, no further test results have been published.

### Conclusions

The methods for determining liquid-side mass-transfer coefficients belong to two main groups: physical absorption or desorption of a poorly soluble gas and chemical absorption. With a solute of very low solubility the liquid-side mass transfer resistance becomes dominant while that of the gas-side can be neglected. If the gas phase is purely the solute, then the gas-side resistance is completely eliminated, at the risk however of rapidly saturating the liquid phase. If the gas-side resistance is not negligible, it is possible to determine both  $k_G a_e$  and  $k_L a_e$  based on assumptions on their dependence to gas and liquid flow rates, but this method is not recommended, as it likely introduces additional errors.

Physical absorption or desorption of CO<sub>2</sub> and O<sub>2</sub> into water are the most popular methods as these solutes have very low solubility and have well established analytical methods. In the case of physical absorption, the useful bed height is more limited due to saturation and uncertainties on the equilibrium value, whereas with desorption the measurement error is only determined by the precision of the analysis.

Chemical absorption, although less common than the above methods, has been used with various reaction systems covering the different regimes. Systems in the instantaneous and slow regimes seem to yield more precise results than those in the intermediate regime, which involves using Danckwerts' plots to determine  $a_e$  from the slope and  $k_L$ , with rather large uncertainties, from the intercept. The magnitude of the gas-side resistance must be checked, as it is not always negligible, and the validity of the applied reaction regime must be verified, which requires some knowledge of the kinetics.

More recently, x-ray tomography has also been proposed to measure local solute concentrations in the liquid phase and determine  $k_L$ , but results are not available at this time.

The choice of the most appropriate method to determine  $k_L$  depends on the packing characteristics, bed geometry and fluids available. When the packed bed NTU<sub>L</sub> is low (small bed heights or low  $k_L a$ ) we recommend desorption as it does not call for the use of thermochemical parameters if the solubility is low. Preferred systems are oxygen from water into N<sub>2</sub> if the latter is available in sufficient quantity, otherwise CO<sub>2</sub> from water into air or N<sub>2</sub>, or toluene from water into air although this solute has toxicity issues. When the bed NTU<sub>L</sub> is large (tall beds and large  $k_L a$ ), then the solute depletion in the liquid phase can become excessive and lead to high measurement uncertainties. In such cases, the chemical absorption of CO<sub>2</sub> added to air into MDEA solutions may offer a reliable method provided the thermochemical parameters are well established.

### Treatment of Internal and External End Effects

The aim of the methods presented above is to determine the mass transfer parameters of packing under fully developed flow conditions. However, depending on how the column is configured, three secondary sources of mass transfer can be

identified that distort the measurement. One takes place in the regions between the packing ends and the gas/liquid sampling positions for chemical analysis and is referred to as the external end effects, the values of which depend on the column configuration, distributor performance and the type of packing. A second takes place in the free ends of the packed bed or of the packed element where the gas (at the bottom) and the liquid (at the top) flow regimes are not yet well established. These regions will change the packing efficiencies, generally in an adverse manner, and are referred to as the internal or entrance (end) effect.<sup>150</sup> Their impact will depend on the performance of the distributor as well as on the self-distribution capability and channeling tendency of the packing. The external and internal end effects are almost always treated together under the name "end effects." Their magnitude depends on the gas and liquid flow rates<sup>71</sup> and, depending on the situation, may vary from only a few percent to more than half of the total absorption.<sup>111</sup> Several authors neglect end effects, by simply stating that they are minimized by the column configuration and distributors used. In view of the potentially high impact of end effects, it is strongly recommended to evaluate them.

The third source of secondary mass transfer is generated by the liquid film along the walls of the column, the contribution of which will decrease with diameter roughly as  $1/D_c$ . Vidwans and Sharma<sup>28</sup> recommend for random packings that the column diameter should be at least eight times the packing size in order to obtain representative values of  $a_e$ . Fair<sup>151</sup> states that wall effects become negligible for diameters larger than 0.6 m.

There is some evidence that the magnitude of end effects also depends on the chemical system, for example, Yoshida and Koyanagi<sup>71</sup> measured higher end effects for vaporization than for physical absorption. The difference decreased with increasing  $L$ , and above certain liquid flow rates, end effects became constant. Higher end effects for vaporization might be explained by a difference in the effective interfacial area of the liquid outside the packed bed.

Experimentally, the end effects can be quantified by either taking samples at different locations of the column, or by performing measurements with multiple packed bed heights. With samples immediately below and above the packings (e.g., Molstad et al.<sup>107</sup>; Vivian and Whitney<sup>99</sup>; Houston and Walker<sup>111</sup>; Weiland et al.<sup>40</sup>; Kolev et al.<sup>19</sup>; Kunze et al.<sup>10</sup>), the mass transfer taking place outside of the column can be measured. However, the internal effects are not eliminated. To overcome this problem, samples can be taken within the packing<sup>4,9,39,54,57,120,152</sup> as well. This procedure assumes that the sampling system inside the packing does not significantly perturb the flow and hence the mass transfer rates in the packing.

Repeating experiments with at least two different packing heights is easier to realize, but the applicable height can be limited for certain measurement methods, such as vaporization of a pure liquid. Instead of actually changing the height of the bed, some authors (e.g., Danckwerts and Gillham<sup>60</sup>; Alper<sup>35</sup>) vary packing height by allowing the bottom of the column to fill up with liquid at different, controlled heights. The location of the gas inlet is varied accordingly, so as to be immediately above the liquid seal. The surface of the liquid, however contributes to the end effects.

The end effects are sometimes regarded as a virtual layer of packing with an equivalent packed bed height ( $H_E$ ). This approach is not theoretically sound, as the dependency of  $H_E$

on  $G$  and  $L$  might not be the same as for the packing.<sup>71,93</sup> The equivalent bed height can be determined by trial and error<sup>91,93</sup>: it is the extra packed bed height that has to be added to the physical one to bring the results of different bed heights into agreement.

The calculation of the true mass-transfer coefficient, when different packing heights are used, is based on the following equation:

$$NTU'_{OG} = NTU_{OG} + NTU_E \quad (52)$$

where the prime sign denotes the NTU measured, the unmarked NTU is that of the packing without the end effects, and  $NTU_E$  is the end effects. If experiments are performed for two heights  $H_2$  and  $H_1$ , the true NTU is obtained for the packing height  $H_2 - H_1$  as<sup>65</sup>:

$$(NTU_{OG})_{2-1} = \frac{H_2 - H_1}{HTU_{OG}} = (NTU'_{OG})_2 - (NTU'_{OG})_1 \quad (53)$$

An alternative equation to calculate the true HTU from the measured HTU values was given by Lynch and Wilke<sup>87</sup>:

$$HTU_{OG} = \frac{(HTU'_{OG})_2 (HTU'_{OG})_1 (H_2 - H_1)}{H_2 (HTU'_{OG})_1 - H_1 (HTU'_{OG})_2} \quad (54)$$

The end effects  $NTU_E$  can be calculated as the difference of the measured and the true NTU of the same packed bed height, or directly with the following equation<sup>71</sup>:

$$NTU_E = \frac{H_1 (NTU'_{OG})_2 - H_2 (NTU'_{OG})_1}{H_1 - H_2} \quad (55)$$

If more than two heights were used, they can simultaneously be taken into account by plotting the measured  $(K_G a_e)'$  vs.  $1/H$ .<sup>86,90,112</sup> By transforming the basic equation, we can obtain:

$$(K_G a_e)' = K_G a_e + NTU_E G \frac{1}{H} \quad (56)$$

A straight line fitted on the measurement points intercepts the ordinate at the true value of the mass-transfer coefficient, while  $NTU_E$  can be calculated from the slope of the line.  $H_E$  can be obtained as the distance between the origin and the intercept of the fitted line with the abscissa.<sup>90,112</sup> For two packing heights, this method gives the same results as the ones presented earlier. All of these methods assume that the true HTU is independent of the height of the packed bed, that is, all the variation of HTU with  $H$  is due to the existence of additive end effects.

The existence of internal effects, however, means that efficiency is not constant in the inlet zones of the packing; therefore, the change of NTU with the packed bed height is not linear for low  $H$  values (Figure 6<sup>150</sup>). If NTU is measured at two heights  $H_1$  and  $H_2$  at the linear part of the curve, the previously presented methods can be used to determine the end effects  $NTU_E$  that is the sum of the external end effect  $NTU_{EE}$  (NTU measured without packing) and the internal end effect  $NTU_{IE}$ . However, if measurements are performed at the non-linear part of the curve, the end effects will be underestimated, and the mass-transfer coefficient overestimated.

Among other approaches to treat end effects, Nakov and Kolev<sup>119</sup> placed a liquid redistributing bed above the packing to be measured. They assumed the end effects to be equal to the mass transfer measured only in the presence of the redistributing layer. In this way, only the external effects are corrected, but the absorption in the redistributing layer is likely to

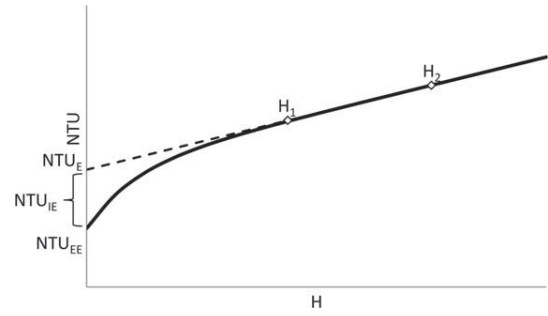


**Figure 6. The change of NTU with the height of the packed bed; the internal ( $NTU_{IE}$ ) and external ( $NTU_{EE}$ ) effects (based on Billet<sup>150</sup>).**

be much higher than the internal effects. Wang et al.<sup>5</sup> measured the mass transfer rates in the column sections below and above the packing, and expressed these (external) end effects as  $NTU_E$ . They found that wall and end effects could be more important for coarser structured packings. Others have estimated end effects not by measurements but by calculation. For instance, Tsai<sup>153</sup> took end and wall effects into account for the determination of  $a_e$  by subtracting their contribution to  $a_e$  from the measured value. The  $a_e$  attributed to the column sections below and above the packing was calculated on the basis of the work of Yeh,<sup>154</sup> by treating these sections as spray columns with spray impacting a solid surface (above the packing), or into a liquid (below the packing). The contribution of the wall to  $a_e$  was calculated by assuming complete wetting. Roesler and Raynal<sup>63</sup> and Alix and Raynal<sup>155</sup> took the wall effect into account by using the  $a_e/a'_g$  ratio, instead of simply  $a_e$ , where  $a'_g$  contains the specific superficial area of the column wall, as well:

$$a'_g = (a_g)_{\text{packing}} + \frac{4}{D_c} \quad (57)$$

This approach assumes that the wettability of the packing and the wall is identical. In fact, it is implicitly assumed that the same fraction of the geometrical surface is effective.

In conclusion, while end effects can be reduced by choosing an appropriate column configuration, it is nonetheless recommended that they be assessed as they can significantly contribute to the overall mass flux. Experimentally this can be performed by taking fluid samples immediately after the packing inlet and exit planes, or even within the packing, in addition to taking fluid samples at the inlet and outlet of the column. Alternatively, at least two different packed bed heights can be used.

### Influence of Packed Bed Height

It is often assumed that the intrinsic mass transfer parameters are independent of the packed bed height, and that measured variations are due entirely to the end effects. The literature is, however, contradictory on this issue with some studies finding a dependency of these intrinsic mass transfer parameters to bed height<sup>41,73,89,110,124,129,138,147,156</sup> and others not reporting any.<sup>30,60,98</sup> The evolutions along the bed most likely originate from flow pattern changes particularly for the liquid. The initial flow pattern will depend on the type and position of the liquid distributor. Further along the bed, the ratio of the packing size and column diameter ( $D_c/D_p$ ), the ratio of the bed height and column diameter ( $H/D_c$ ), the

packing type, hydraulic loads and liquid properties will affect the liquid flow distribution. This section describes the phenomena affecting the liquid flow and the impact on mass transfer parameters.

### ***Evolutions of the liquid flow distributions along packed beds***

The liquid entering the packed bed has an initial distribution, whose quality is determined by the liquid distributor. A good initial distribution (which is usually, but not always a uniform one<sup>138</sup>) neither leaving a large part of the packing dry, nor leading to excessive wall flow, is important for proper functioning of the column.

The liquid flowing down the packed bed will establish a stabilized distribution pattern only after a certain distance from the liquid distributor (1–2 packing layers for structured packings), and thus there exists a minimum packed bed height necessary to measure height-independent mass transfer parameters. Maćkowiak and Maćkowiak<sup>16</sup> recommend a  $H/D_c$  ratio higher than 2.5, and a bed height exceeding 1 m.

The quality of liquid distribution can deteriorate with increasing bed height. This maldistribution phenomenon is defined as a deviation of the real flow pattern from the plug flow used in most column models. Maldistribution may be generated at the inlet due to the distributor or throughout the bed owing to the nature of the packing. Excessively long packed beds should therefore not be used: in industrial columns liquid redistribution generally becomes necessary after 2–3 m height (15–20 theoretical stages), although well-functioning columns with packed beds higher than 10 m packing exist.<sup>157</sup> Maldistribution can manifest itself in axial mixing, in incomplete wetting of some parts of the packing, and in the tendency of the liquid to spread toward the wall of the column, and once reaching it, to flow along the wall. Wall flow is undesirable, as it reduces the effective interfacial area of the column, and changes the local  $L/G$  ratio, although  $k_G$  and  $k_L$  may increase through intensive mixing where the packing elements touch the wall.<sup>138</sup> A high  $D_c/D_p$  ratio helps to avoid excessive wall flow. The following values are recommended (see also the section “Standardization”):  $D_c/D_p \geq 10$  for random packings,<sup>8</sup>  $D_c \geq 200$  mm for structured packings.<sup>158</sup> For random packings, liquid spreading is rather limited particularly with smaller  $D_p$ . In the case of structured packings, however, the ordered structure allows radial spreading of the liquid. Wall wipers, on the other hand, reduce wall flow by redirecting the liquid toward the packing. Denser packings (such as random packings) may be less sensitive to the increase of  $H$ .<sup>41</sup> For more information on maldistribution, the reader is referred to the book of Górak and Olujić.<sup>159</sup> Brunazzi and Paglianti<sup>147</sup> pointed out that the effect of the packed bed height cannot be solely attributed to liquid maldistribution if mixing in the contact points between packing elements is incomplete.

### ***Mass transfer parameter evolutions with bed height***

The experimental results indicating an influence of packed bed height will be discussed in the following sections. Results on the effect of column diameter are also included. With two exceptions,<sup>41,148</sup> all the experiments were performed with random packings. In all the cases, if a dependency was observed, the mass transfer parameters decrease with increasing packed bed height, and increase with increasing column diameter.

**Effective Interfacial Area.** The evidence of the effect of  $H$  on the interfacial area is scant. Yoshida and Koyanagi<sup>73</sup> performed experiments with two packed bed heights, and found that  $a_e$  was higher for the shorter packed bed. This could be explained by different magnitudes of end effects and/or by worse liquid distribution in the higher bed. Based on the experimental work available in the literature on the determination of  $a_e$  by chemical absorption, Charpentier<sup>14</sup> concluded that in the trickle flow regime  $a_e$  is independent of  $H$ , but increases with  $D_c$ . Henriques de Brito et al.<sup>41</sup> found with Mellapak 125.Y that  $a_e$  is reduced by increasing  $H$ . The magnitude of reduction, however, depends on  $L$ , and is greater for low liquid loads. The authors explain this by a stronger influence of channeling effects at lower flow rates. Based on distillation results, Bravo and Fair<sup>67</sup> proposed a correlation in which  $a_e$  is proportional to  $H^{-0.4}$  for random packings. From the above literature the effect of bed height, if any, is generally to degrade the effective area.

**Gas-Side Mass-Transfer Coefficient.** Studies dealing with the dependency of the gas-side mass transfer parameter on  $H$  are also scarce. Van Krevelen et al.<sup>89</sup> found that  $k_G$  is proportional to  $(D_c/H)^{1/3}$ . Molstad and Parsly<sup>110</sup> concluded on the basis of previous measurements that unlike  $k_L a_e$ ,  $k_G a_e$  is dependent on  $H$ , being approximately proportional to  $H^{-1/3}$ .

Correlations found in the literature generally do not take the packed bed height into account. Exceptions include the correlation of Wagner et al.,<sup>160</sup> developed for distillation with random packings, which gives  $k_G$  as proportional to  $H^{-0.5}$ , and those of Piché et al.,<sup>161,162</sup> which were obtained with the use of artificial neural networks based on an extensive database of absorption measurement results.

**Liquid-Side Mass-Transfer Coefficient.** More extensive research on the effects of bed height has been conducted concerning the liquid-side mass-transfer coefficient. Van Krevelen and Hoftijzer<sup>124</sup> found that  $k_L$  is proportional to  $(D_c/H)^{1/3}$ , just as for  $k_G$ . According to Fujita et al.,<sup>156</sup>  $k_L a_e$  is proportional to  $H^{-0.19}$ . Yoshida and Koyanagi<sup>73</sup> observed an increase in  $HTU_L$  with  $H$  that they considered too high to be explained only by the existence of end-effects, and they supposed that  $k_L a_e$  decreases with increasing  $H$ . Cornell et al.<sup>163</sup> suggested an exponent of  $-0.15$  based on the evaluation of experimental results of several authors. However, as results from different sources are used, this value might have a significant error. An effect of  $D_c$  was not observed.

The aim of Hikita et al.<sup>130</sup> was to clarify whether  $H$  has an effect on  $HTU_L$  or not. The authors performed experiments with two columns (diameters: 6.6 and 12.5 cm) using Raschig rings with bed heights between 0.05 and 1.50 m. They found that  $H$  had no effect in the larger diameter column. In the case of the smaller column, the authors classified three regions (A, B, and C) on a map of  $H$  vs.  $L$ . Region A was for high flow rates, Region B for low flow rates with short beds or medium flow rates with higher beds, while Region C was for low flow rates and high beds. The packed bed height had no effect in Region A, while  $HTU_L$  was proportional to  $H^{0.08}$  in Region B and with  $H^{0.44}$  in Region C. The effect of  $H$  is explained by the authors as the result of the potential non-uniformity of the liquid distribution.

Mangers and Ponter<sup>138</sup> found that  $k_L a_e$  decreased with increasing  $H$  (varied between 25 and 75 cm) both for readily and poorly wettable ring packings. They also measured the ratio of wall flow to total flow as a function of  $H$ , and the

increase of wall flow with  $H$  can be an explanation of the diminishing  $k_L a_e$ .

Brunazzi and Paglianti<sup>147</sup> state that increasing  $H$  decreases  $k_L$  if mixing at the contact points between packing elements (called junctions by the authors) is incomplete, both in the case of random and structured packings. As shown experimentally and theoretically by Nawrocki and Chuang<sup>164</sup> for absorption into stable rivulets on an inclined plate, the flow distance of the liquid influences considerably the mass transfer. In the case of complete mixing, the flow distance is a function of geometry of packing elements, for example, that of channel dimensions for structured packings. If partial mixing occurs, the flow distance is the distance covered by the liquid from the top to the bottom of the column, which is certainly related not only to packing dimensions, but to the packed bed height, as well. The effect of  $H$  was observed only at  $H > 1$  m, and below a critical  $Re_L$  value (100). The column diameter was 10 cm; the packings used were Sulzer BX and Mellapak 250.Y. Note that these findings are in accordance with results of Hikita et al.,<sup>130</sup> and suggest that not only the packed bed height, but also the liquid flow rate is important.

As in the case of  $k_G$ , correlations generally do not contain  $H$  as a parameter. Exceptions are the correlation of Wagner et al.<sup>160</sup> in which  $k_L$  is proportional to  $H^{-0.5}$  for random packings, that of Brunazzi and Paglianti,<sup>147</sup> and those of Piché et al.<sup>161,162</sup> obtained with the use of artificial neural networks.

## Standardization

As pointed out in the introduction of the article, the often strong variation of experimental data on mass-transfer coefficient obtained from different sources with the same packing calls for the standardization of the measurement methods. More reliable and comparable mass transfer parameters could lead to a reduction of safety factors in column design, and thus a reduction of investment and operating costs.<sup>10</sup> However, unlike for distillation, no standard has been established for absorption.

Hoffmann et al.<sup>8</sup> recommended the use of the following chemical systems: absorption of low concentration  $CO_2$  in aqueous NaOH solutions for  $a_e$ , absorption of  $SO_2$  into NaOH solutions for  $k_G$ , absorption of  $NH_3$  in water for  $k_L$ . The desorption of  $CO_2$  from water is mentioned as an alternative to measure  $k_L$ , but it was not applied by the authors. Both by the determination of  $a_e$  and  $k_L$ , the gas-side resistance was taken into account by subtracting its value, calculated on the basis of the  $SO_2$  absorption measurements, from the overall resistance. The relative error was the highest in the case of  $a_e$ , as it reached values of 30%. This error propagated to  $k_G$  and  $k_L$  as well through the division of  $k_G a_e$  and  $k_L a_e$  by  $a_e$ .

Hoffmann et al.<sup>8</sup> state that the physical properties must have high accuracy in order to reduce the error of the evaluation. They have selected a set of properties from the literature deemed to be most accurate for the systems used. Concerning the experimental setup, they have defined the following set of requirements:

- Isothermal experiments to avoid variations of system properties. This can be achieved by performing experiments at room temperature, using heating jacket and tempering the feed streams.
- Minimization of wall effects to ensure reliable scale-up data. For structured packings  $D_c$  should be higher than 20 cm (as recommended by Olujić<sup>158</sup>) for random packings the ratio  $D_c/D_p$  should be higher than 10.

- Minimization of evaporation by pre-saturation of the gas flow in order to ensure single component mass transfer.

- Uniform initial gas and liquid distribution to avoid maldistribution and inlet effects by installing suitable and technical relevant gas and liquid distributors ( $>100$ – $200$  drip points/ $m^2$  for industrial scale).

- Consideration of absorption in the bottom of the column to account for end effects at the bottom of the column by measuring fluid compositions both at the column bottom inlet/exit and directly below the packing.

- Measurable outlet gas composition (in the case of absorption) to ensure mass transfer along the complete column height, that is, avoiding the depletion of the solute in the gas phase. This can be achieved by adjusting the packing height or by using sufficiently high solute concentration in the inlet gas.

- Use of one uniform packing height for comparison with different test systems to eliminate the effects of packing height differences.

- Standardized filling method to avoid maldistribution and undefined packing structure. In order to be able to compare results, the structure of the packed bed should not show significant variation between different measurements. The average void fraction of the bed describes the packing density. However, local variations of the structure, and thus the void fraction, can induce maldistribution, and thus change the results of mass transfer measurements even if the average packing densities are identical. Measuring the dry pressure drop of the bed gives information on the structure of the bed. Measurement of the concentration profile along the column height<sup>165–167</sup> can help identifying local variations in the structure of the bed.

- Representative gas and liquid samples. The composition can vary over the column cross-section. By determining gas and liquid profiles over the column cross-section, a uniform distribution can be ensured. Measurement of composition in the inlet and outlet tubes is also recommended.

Hoffmann et al.<sup>8</sup> also recommend that when publishing new mass transfer correlations, researchers give the following information, as well:

- Fluid systems along with their physical and chemical properties,
- Experimental setup ( $D_c$ ,  $H$ , packing geometry),
- Experimental procedure, number of data points, range of gas, and liquid loads,
- Processing method, analytical techniques, and uncertainties,
- Validity range of the proposed correlation (physical properties and loading conditions).

Rejl et al.<sup>9</sup> performed an assessment of the recommendations of Hoffmann et al.<sup>8</sup> They recommend the use of systems where the mass transfer resistance is only present in one phase. In view of this,  $k_L a_e$  was proposed to be measured using the absorption or desorption of  $CO_2$  or  $O_2$  in/from water, instead of the absorption of  $NH_3$ , where as much as 50% might lie in the gas phase. Moreover, Hoffmann et al.<sup>8</sup> calculated  $k_L$  with the assumption that interfacial area measured by the absorption of  $CO_2$  (chemical absorption) is equal to that of the absorption of  $NH_3$  (physical absorption). For the determination of  $k_G$  and  $a_e$ , Rejl et al.<sup>9</sup> recommend the same systems as Hoffmann et al.<sup>8</sup> In the case of  $a_e$ , a gas velocity higher than 0.5 m/s and a  $OH^-$  concentration less than 1 mol/L are recommended, in order to make the gas-side resistance negligible.

The physical properties used should be the same as those used originally in the evaluation of the kinetic constant. The end-effects should be eliminated by taking samples directly from the packing. In the case of absorption, low outlet gas-phase solute concentrations may introduce significant error in the mass transfer parameters. To prevent this from happening, the packed height should be limited such that the gaseous solute is not depleted beyond 95% of its entrance level. The authors also investigated the effect of axial dispersion using 25 mm metal Pall rings and found that, when it is taken into account,  $k_G a_e$  values are 10–15% higher while  $k_L a_e$  can be up to 30% higher at low liquid loads. These dispersion effects are comparable in magnitude to the scatter among literature data for a given packing. Rejl et al.<sup>9</sup> also point out that the disparity in  $k_L$  and  $k_G$  values is significantly lower for measurements performed in a given laboratory, than in different ones, which hints at the possible benefits of using a set of standardized methods to determine the mass-transfer coefficients.

The review of Schultes<sup>168</sup> on mass transfer columns research also identified the definition of test facility setup standards as one of the future research tasks. As demonstrated by measurement results from the literature, the performance of column internals depend significantly on the experimental setup and on the institute where the work has been done. The different correlations often give different results, as well. The gas- and liquid-side mass-transfer coefficients are expected to have  $\pm 10\%$  deviation between measured data and values predicted with state-of-the-art correlations (e.g. Billet and Schultes<sup>169</sup>) if measurements were performed on the same column with a specific packing. If multiple data sets (absorption, desorption, rectification) are used to calculate the mass-transfer coefficients,  $\pm 20\%$  mean deviation can be expected. In the case of extrapolation for different physical properties or flow rates, deviations can be around  $\pm 50\%$ . The value of  $a_e$  is even less accurate, with  $\pm 80\%$  mean deviation for interpolation and more than  $\pm 100\%$  for extrapolation.

Maćkowiak and Maćkowiak<sup>16</sup> give the following recommendations on the experimental setup. The column diameter should be high enough so that  $D_c/D_p > 10$ . Either the packed bed height should be higher than 1.0 m, or the ratio  $H/D_c$  should be higher than 2.5 to minimize maldistribution.

Wolf et al.<sup>170</sup> investigated the effect of experimental setup on the mass transfer measurements. Multiple sampling locations were studied both for the gas and the liquid phase. The authors recommended taking integral samples over the whole cross section of the column immediately above and below the packing. They also reported that  $HTU_{OG}$  and  $HTU_{OL}$  depend on the solute concentration. These authors called for a detailed pre-treatment procedure to ensure comparability of the results, specifically with plastic packings as their wettability increases with time until reaching a stable value. Their results showed stabilization after four cycles of irrigation and absorption (4 h of total time). Billet and Maćkowiak<sup>139</sup> reported that the packing efficiency and pressure drop became constant after one week of operation. Maćkowiak and Maćkowiak<sup>16</sup> also recommended the pre-treatment of plastic packings.

Kunze et al.<sup>171</sup> outlined a collaborative project with two academic and several industrial partners, including packing vendors and end users with the aim of developing standards for mass transfer measurements in absorption and desorption, for both experimental apparatus and evaluation methods. In view of rate-based simulation results, the effect of

experimental configuration, and that of the possible measurement errors are also to be evaluated. Similarly to Hoffmann et al.,<sup>8</sup> the authors propose the pre-saturating the gas phase with water in a saturator column. As for the chemical systems they repeat the recommendations of Rejl et al.<sup>9</sup> with the addition of the absorption of  $NH_3$  in aqueous  $H_2SO_4$  (also an instantaneous reaction) for  $k_G$ . For the determination of  $k_L$ , they recommended using desorption of  $CO_2$  or  $O_2$  from water, while Rejl et al.<sup>9</sup> considered absorption, as well. These systems satisfy the criteria for the location of mass transfer resistance required for evaluating the associated mass transfer parameter. In selecting the systems, other criteria must be taken into account as well, such as ease of analysis, accuracy of physical properties, environmental and safety risks, availability, and price. The physical properties have to be calculated in a standardized way, as well.

As a result of the above project, Kunze et al.<sup>10</sup> proposed a standardized measurement procedure and mass transfer parameter determination. The systemic, step-wise determination of the parameters was described, using three chemical systems to determine  $k_G$ ,  $k_L$ , and  $a_e$ . The recommendations of Kunze et al.<sup>171</sup> were reasserted, with the addition of a positive viewpoint on the use of toluene desorption from water into air, as an alternative to measure  $k_L a_e$ . To take into account the gas-side resistance on the determination of  $a_e$ , three possibilities were mentioned: (1) to neglect the resistance, (2) to calculate  $k_G$  from published correlations, (3) to calculate  $k_G$  from  $k_G a_e$  measured by the same researchers. The first possibility could be useful to quickly compare  $a_e$  of different packings. The second option is especially interesting if the correlation was determined by the standardized methods, or by another method that is transparent and comprehensible. Otherwise, the third option is suggested, that is, using data from the same source. For test systems, calculation methods for the determination of physical and chemical properties were recommended. A sensitivity analysis highlighted that the measured concentrations and volumetric flow rates have the highest influence on the accuracy of mass-transfer coefficients, while the influence of pressures and temperatures is lower.

Kunze et al.<sup>10</sup> also presented a case study of the proposed method, including the experimental setup, process measurements and samplings. Gas and liquid samples were taken directly below and above the packing, however, end effects were not discussed. Instead of using a pre-saturator column, the gas phase was recirculated in order to ensure its saturation with water vapor. The experimental details can be found in the project report, which is also accompanied by a software with which measurement can be evaluated.<sup>172</sup>

As presented in this section, the issue of standardizing mass transfer measurements in absorption has been treated by multiple authors in recent years. The proposition of Kunze et al.<sup>10</sup> is particularly interesting, as it is backed by several industrial partners. However, all the authors implicitly assume that the effective interfacial area are the same for the three chemical systems used to determine the mass transfer parameters. This assumption is likely to be true for the methods used to determine  $a_e$  and  $k_G a_e$ : both use chemical absorption with an excess of liquid phase reagent, and the saturation of certain liquid zones can be neglected. On the other hand, it is not clear to which extent  $a_e$  is reduced by the depletion of dissolved gas in stagnant or semi-stagnant liquid zones in the case of desorption, applied to determine  $k_L a_e$ .

## Conclusions

Measurement methods of interfacial areas ( $a$ ), gas- ( $k_G$ ) and liquid-side ( $k_L$ ) mass-transfer coefficients have been reviewed for packed absorption columns. The methods reviewed range from the earliest experiments to the most recent ones thus providing a broad overview of the possibilities and offering opportunities to reassess older methods in light of modern measurement techniques. In recent years, several authors have called for the standardization of measurement methods for absorption, and our work aims to contribute to this effort.

There exists a wide variety of techniques for specific area measurements. However, the various techniques do not all represent the same surfaces. Evaporation methods will give the true gas-liquid interfacial area whereas physical absorption or desorption methods will give an effective interfacial area which will be lower in value due to the existence of stagnant regions. It is important to clearly distinguish these different types of areas in order to use the appropriate one for column design. The most common method is one that is also recommended for standardization by several authors, namely the absorption of  $\text{CO}_2$  into  $\text{NaOH}$  solutions. This system yields the effective area for chemical absorption. A new, albeit costly alternative is x-ray tomography which has the potential of providing very localized on top of global information.

In practice,  $k_G$  and  $k_L$  cannot be measured directly, but only from mass-transfer coefficients measurements of  $k_{Ga_e}$  and  $k_{La_e}$  after division by the appropriate effective area. Methods for determining the gas- or liquid-side mass-transfer coefficients are based on global flux measurements with systems that attempt to minimize the contribution of the resistance of the other phase to the measured global flux. For  $k_{Ga}$ , this can happen by evaporating a pure liquid, by the absorption of a highly soluble gas or by using a very fast chemical reaction which takes place on the gas-liquid interface (e.g.,  $\text{SO}_2$  and  $\text{NaOH}$ ). For  $k_{La}$ , the gas side resistance is minimized by using poorly soluble solutes under conditions of absorption or desorption, such as with  $\text{CO}_2$ ,  $\text{O}_2$ , or even toluene in water. Less frequently, chemical absorption is also used in different reaction regimes.

The treatment of internal and external end effects needs to be considered in order to evaluate the intrinsic mass transfer parameters of the packings. These can be negligible with tall beds, but significant with short beds. The latter ones are encountered specifically in the determination of  $k_{Ga}$  because the  $\text{HTU}_G$  in packings is generally small. Short beds are also encountered with  $k_{La}$  under absorption conditions due to the rapid approach to equilibrium. Since the magnitude of end effects can sometimes be very significant, it is recommended that they be determined by using multiple packed bed heights, or to make fluid composition measurements from fluid samples taken inside the packing or at least very close to the inlet and outlet planes. Even if end effects are eliminated, the mass transfer parameters can be influenced by the packed bed height. The most likely cause of this is liquid phase maldistribution that will modify the measured parameters, even if height dependency is not observed. By choosing a correct experimental setup, maldistribution can be avoided or reduced.

Finally, the suggestions for standardization of measurement methods were also reviewed. The recommendations of the authors cover test systems, experimental setup and procedures, analytical methods, and data treatment in order to ensure reliable and comparable measurement results. Standardization

will be a great step in reducing the scatter of data measurements among test centers and will lead to more reliable mass transfer parameter correlations.

## Notation

### Roman letters

- $A$  = absorbed component, solute
- $A^*$  = concentration of the solute at the surface of the liquid phase without chemical reaction,  $\text{mol}/\text{m}^3$
- $A^0$  = concentration of the solute in the bulk liquid,  $\text{mol}/\text{m}^3$
- $a$  = specific area,  $\text{m}^2/\text{m}^3$
- $B$  = the reagent in the liquid phase
- $B^0$  = concentration of the reagent in the bulk liquid,  $\text{mol}/\text{m}^3$
- $C$  = factor by which the reaction increases the absorption capacity per unit volume of the liquid
- $D$  = diffusion coefficient,  $\text{m}^2/\text{s}$
- $D_c$  = diameter of the column, m
- $D_p$  = packing size, m
- $E$  = enhancement factor
- $G$  = molar flux of gas,  $\text{mol}/(\text{m}^2\cdot\text{s})$
- $H$  = packed bed height, m
- $Ha$  = Hatta number
- $He$  = Henry's law constant
- HETP = height equivalent of theoretical plate, m
- HTU = height of one transfer unit, m
- $K_G$  = gas-side overall mass-transfer coefficient,  $\text{mol}/(\text{m}^2\cdot\text{s})$
- $K_L$  = liquid-side overall mass-transfer coefficient,  $\text{mol}/(\text{m}^2\cdot\text{s})$
- $k$  = rate constant ( $\text{m}^{3(m+n)}/\text{mol}^{(m+n-1)}$ )
- $k_G$  = gas-side mass-transfer coefficient,  $\text{mol}/(\text{m}^2\cdot\text{s})$
- $(k_Ga)_L$  = gas-side volumetric mass-transfer coefficient at the liquid superficial velocity corresponding to completely wetted packing,  $\text{mol}/(\text{m}^2\cdot\text{s})$
- $k_L$  = liquid-side mass-transfer coefficient,  $\text{mol}/(\text{m}^2\cdot\text{s})$ , in Figure 1: 1/s
- $k_{L,R}$  = liquid-side mass-transfer coefficient in presence of a chemical reaction,  $\text{mol}/(\text{m}^2\cdot\text{s})$
- $k_R$  = reaction term, 1/s
- $L$  = mass flux of liquid,  $\text{kg}/(\text{m}^3\cdot\text{h})$
- $l$  = volume of liquid phase per unit volume of packing
- $m$  = order of reaction with respect to the solute (section "Determination of the Effective Interfacial Area") equilibrium relation between gas and liquid phase mole fraction (elsewhere)
- $n$  = order of reaction with respect to the liquid phase reagent
- NTU = number of transfer units
- $p$  = coefficient in Eq. 30 (section "Determination of the Gas-Side Mass-Transfer Coefficient—Physical absorption") partial pressure of the solute in the bulk gas (elsewhere; Pa)
- $q$  = coefficient in Eq. 30
- $r$  = coefficient in Eq. 30
- Re = Reynolds number
- Sc = Schmidt number
- $u$  = superficial velocity, m/s
- $x$  = mole fraction in liquid phase
- $y$  = mole fraction in gas phase

### Greek letters

- $\alpha$  = coefficient in Eq. 30
- $\beta$  = coefficient in Eq. 30
- $\gamma$  = coefficient in Eq. 32
- $\gamma_{DG}$  = ratio of the rates of absorption into reacting and  $\text{CO}_2$ -free inert solution
- $\gamma_{JD}$  = factor used by Joosten and Danckwerts<sup>22</sup>
- $\eta$  = effective part of  $a_{st}$
- $v$  = the ratio of the reacting number of moles of  $B$  and  $A$
- $\Phi$  = rate of absorption per unit volume,  $\text{mol}/(\text{m}^3\cdot\text{s})$
- $\phi$  = rate of absorption per unit surface,  $\text{mol}/(\text{m}^2\cdot\text{s})$

### Subscripts

- cell = stirred cell
- dry = dry surface
- dyn = dynamic
- E = end effect

e = effective  
 EE = external end effect  
 G = gas phase  
 g = geometrical  
 i = interface, interfacial  
 IE = internal end effect  
 in = entering the column  
 inf = infinitely fast reaction  
 L = liquid phase  
 OG = overall gas-side  
 OL = overall liquid-side  
 out = leaving the column  
 st = static  
 w = wetted

### Superscripts

\* = equilibrium  
 ′ = measured

### Literature Cited

- Green DW, Perry RH. *Perry' Chemical Engineers' Handbook*, 8th ed. New York: McGraw-Hill, 2008.
- Wang GQ, Yuan XG, Yu KT. Review of mass-transfer correlations for packed columns. *Ind Eng Chem Res.* 2005;44(23):8715–8729.
- Laso M, Henriques de Brito M, Bomio P, von Stockar U. Liquid-side mass transfer characteristics of a structured packing. *Chem Eng J.* 1995;58:251–258.
- Valenz L, Rejl FJ, Šíma J, Linek V. Absorption mass-transfer characteristics of Mellapak packings series. *Ind Eng Chem Res.* 2011;50:12134–12142.
- Wang C, Perry M, Seibert F, Rochelle G. Packing characterization for post combustion CO<sub>2</sub> capture: mass transfer model development. *Energy Procedia.* 2014;63:1727–1744. doi:10.1016/j.egypro.2014.11.180
- Hanley B, Chen CC. New mass-transfer correlations for packed towers. *AIChE J.* 2012;58:132–152.
- Rocha JA, Bravo JL, Fair JR. Distillation columns containing structured packings: a comprehensive model for their performance. 2. mass-transfer models. *Ind Eng Chem Res.* 1996;35:1660.
- Hoffmann A, Mačkowiak JF, Górák A, Haas M, Löning JM, Runowski T, Hallenberger K. Standardization of mass transfer measurements. *Chem Eng Res Des.* 2007;85(1):40–49.
- Rejl FJ, Linek V, Moucha T, Valenz L. Methods standardization in the measurement of mass-transfer characteristics in packed absorption columns. *Chem Eng Res Des.* 2009;87(5):695–704.
- Kunze AK, Lutze P, Kopatschek M, Mačkowiak JF, Mačkowiak J, Grünewald M, Górák A. Mass transfer measurements in absorption and desorption: determination of mass transfer. *Chem Eng Res Des.* 2015;104:440–452.
- Laurent A, Charpentier JC. Aires interfaciales et coefficients de transfert de matière dans les divers types d'absorbours et de réacteurs gaz-liquide. *Chem Eng J.* 1974;8:85–101.
- Sharma MM, Danckwerts PV. Chemical methods of measuring interfacial area and mass transfer coefficients in two-fluid systems. *Br Chem Eng.* 1970;15(4):522–528.
- Laurent A, Prost C, Charpentier JC. Détermination par méthode chimique des aires interfaciales et des coefficients de transfert de matière dans les divers types d'absorbours et de réacteurs gaz-liquide. *J Chim Phys.* 1975;72(2):236–244.
- Charpentier J. Recent progress in two phase gas—liquid mass transfer in packed beds. *Chem Eng J.* 1976;11:161–181.
- Ahmadi A. Modélisation de l'absorption réactive multiconstituant: application au traitement des gaz acides par des solvants aux alcanolamines. Ph.D. Dissertation, University of Toulouse, Toulouse, France, 2011.
- Mačkowiak J, Mačkowiak JF. *Random packings*. In: Górák A, Olujić Ž, editors. *Distillation: Equipment and Processes*. Amsterdam, The Netherlands: Academic Press, 2014:85–144.
- Tsai RE, Seibert AF, Eldridge RB, Rochelle GT. A dimensionless model for predicting the mass-transfer area of structured packing. *AIChE J.* 2011;57(5):1173–1184.
- Puranik SS, Vogelupohl A. Effective interfacial area in irrigated packed columns. *Chem Eng Sci.* 1974;29:501–507.
- Kolev N, Nakov S, Ljutzkanov L, Kolev D. Effective area of a highly efficient random packing. *Chem Eng Process.* 2006;45:429–436.
- Shulman HL, Ullrich CF, Wells N, Proulx AZ. Performance of packed columns. III. Holdup for aqueous and nonaqueous systems. *AIChE J.* 1955b;1(2):259–264.
- Shulman HL, Savini CG, Edwin RV. Performance of packed columns VII. The effect of holdup on gas-phase mass transfer rates. *AIChE J.* 1963;9(4):479–484.
- Joosten GEH, Danckwerts PV. Chemical reaction and effective interfacial areas in gas absorption. *Chem Eng Sci.* 1973;28:453–461.
- Last W, Stichlmair J. Determination of mass transfer parameters by means of chemical absorption. *Chem Eng Technol.* 2002;25(4):385–391.
- Benadda B, Kafoufi K, Monkam P, Otterbein M. Hydrodynamics and mass transfer phenomena in counter-current packed column at elevated pressures. *Chem Eng Sci.* 2000;55:6251–6257.
- Aroonwilas A, Veawab A. Characterization and comparison of the CO<sub>2</sub> absorption performance into single and blended alkanolamines in a packed column. *Ind Eng Chem Res.* 2004;43(9):2228–2237.
- Danckwerts PV. *Gas-Liquid Reactions*. New York: McGraw-Hill, 1970.
- Yoshida F, Miura Y. Effective interfacial area in packed columns for absorption with chemical reaction. *AIChE J.* 1963;9(3):28–29.
- Vidwans AD, Sharma MM. Gas-side mass transfer coefficient in packed columns. *Chem Eng Sci.* 1967;22:673–684.
- Jhaveri AS, Sharma MM. Effective interfacial area in a packed column. *Chem Eng Sci.* 1968;23(7):669–676.
- Danckwerts PV, Rizvi SF. The design of gas absorbers part ii: effective interfacial areas for several types of packing. *Trans Inst Chem Eng.* 1971;49:124–127.
- Onda K, Takeuchi H, Maeda Y. The absorption of oxygen into sodium sulphite solutions in a packed column. *Chem Eng Sci.* 1972;27(2):449–451.
- Sahay BN, Sharma MM. Effective interfacial area and liquid and gas side mass transfer coefficients in a packed column. *Chem Eng Sci.* 1973;28:41–47.
- Linek V, Stoy V, Machoň V, Krivský Z. Increasing the effective interfacial area in plastic packed absorption columns. *Chem Eng Sci.* 1974;29:1955–1960.
- Linek V, Krivský Z, Hudec P. Effective interfacial area in plastic-packed absorption columns. *Chem Eng Sci.* 1977;32:323–326.
- Alper E. Measurement of effective interfacial area in a packed-column absorber by chemical methods. *Trans Inst Chem Eng.* 1979;57:64–66.
- Merchuk JC. Mass transfer characteristics of a column with small plastic packings. *Chem Eng Sci.* 1980;35:743–745.
- Rizzuti L, Augugliaro V, Lo Cascio G. The influence of the liquid viscosity on the effective interfacial area in packed columns. *Chem Eng Sci.* 1981;36:973–978.
- Neelakantan K, Gehlawat JK. New chemical systems for the determination of liquid-side mass transfer coefficient and effective interfacial area in gas-liquid contactors. *Chem Eng J.* 1982;24:1–6.
- Linek V, Petříček P, Beneš P, Braun R. Effective interfacial area and liquid side mass transfer coefficients in absorption columns packed with hydrophilised and untreated plastic packings. *Chem Eng Res Des.* 1984;62(1):13–21.
- Weiland RH, Ahlgren KR, Evans M. Mass-transfer characteristics of some structured packings. *Ind Eng Chem Res.* 1993;32:1411–1418.
- Henriques de Brito M, von Stockar U, Menendez Bangerter A, Bomio P, Laso M. Effective mass-transfer area in a pilot plant column equipped with structured packings and with ceramic rings. *Ind Eng Chem Res.* 1994;33:647–656.
- Benadda B, Otterbein M, Kafoufi K, Prost M. Influence of pressure on the gas/liquid interfacial area a and the coefficient kLa in a counter-current packed column. *Chem Eng Process.* 1996;35:247–253.
- Weimer T, Schaber K. Absorption of CO<sub>2</sub> from the atmosphere as a method for the estimation of effective interfacial areas in packed columns. *Inst Chem Eng Symp Ser.* 1997;142:417.
- Nakajima ES, Maffia MC, Meirelles AJA. Influence of liquid viscosity and gas superficial velocity on effective mass transfer area in packed columns. *J Chem Eng Jpn.* 2000;33(3):561–566.
- Duss M, Meierhofer H, Bornio P. Bestimmung der effektiven Stoffaustauschflächen bei hoher Flüssigkeitsbelastung für Nutter-Ringe. *Chem Ing Tech.* 2000;72(9):1053.
- Duss M, Meierhofer H, Nutter DE. Effective interfacial area and liquid holdup of nutter rings at high liquid loads. *Chem Eng Technol.* 2001;24(7):716–723.

47. Duss M, Menon A. Optimized absorber design for post-combustion CCS. In: *Proc. of the Distillation and Absorption 2010 Conference*. Eindhoven: Eindhoven University of Technology, 2010:109–114.
48. Nakov S, Kolev N, Ljutzkanov L, Kolev D. Comparison of the effective area of some highly effective packings. *Chem Eng Process*. 2007;46(12):1385–1390.
49. Green CW. *Hydraulic Characterization of Structured Packing via X-Ray Computed Tomography*. Ph.D. Dissertation, University of Texas at Austin, Austin, TX, 2006.
50. Tsai RE, Schultheiss P, Kettner A, Christopher Lewis J, Frank Seibert A, Bruce Eldridge R, Rochelle GT. Influence of surface tension on effective packing area. *Ind Eng Chem Res*. 2008;47(3):1253–1260.
51. Tsai RE, Seibert AF, Eldridge RB, Rochelle GT. Influence of viscosity and surface tension on the effective mass transfer area of structured packing. *Energy Procedia*. 2009;1(1):1197–1204.
52. Alix P, Raynal L. Pressure drop and mass transfer of a high capacity random packing. Application to CO<sub>2</sub> post-combustion capture. *Energy Procedia*. 2009;1(1):845–852. doi:10.1016/j.egypro.2009.01.112
53. Alix P, Raynal L, Abbe F, Meyer M, Prevost M, Rouzineau D. Mass transfer and hydrodynamic characteristics of new carbon carbon packing: Application to CO<sub>2</sub> post-combustion capture. *Chem Eng Res Des*. 2011;89(9):1658–1668.
54. Aferka S, Viva A, Brunazzi E, Marchot P, Crine M, Toye D. Tomographic measurement of liquid hold up and effective interfacial area distributions in a column packed with high performance structured packings. *Chem Eng Sci*. 2011;66(14):3413–3422.
55. Wang C, Perry M, Rochelle GT, Seibert AF. Packing characterization: mass transfer properties. *Energy Procedia*. 2012;23:23–32.
56. Wang C, Perry M, Seibert F, Rochelle GT. Characterization of novel structured packings for CO<sub>2</sub> capture. *Energy Procedia*. 2013;37:2145–2153.
57. Rejl FJ, Valenz L, Haidl J, Kordač M, Moucha T. Hydraulic and mass-transfer characteristics of Raschig Super-Pak 250Y. *Chem Eng Res Des*. 2015;99:20–27.
58. Deckwer WD. *Bubble Colum Reactions*. Chichester, UK: John Wiley & Sons, 1992.
59. Pohorecki R, Moniuk W. Kinetics of reaction between carbon dioxide and hydroxyl ions in aqueous electrolyte solutions. *Chem Eng Sci*. 1988; 43:1677–1684.
60. Danckwerts PV, Gillham AJ. The design of gas absorbers, I—methods for predicting rates of absorption with chemical reaction in packed columns, and tests with 11/2 in. Raschig rings. *Trans Inst Chem Eng*. 1966;44:T42.
61. Rizzuti L, Augugliaro V, Marrucci G. Ozone absorption in alkaline solutions. *Chem Eng Sci*. 1976;31:877–880.
62. Rizzuti L, Brucato A. Liquid viscosity and flow rate effects on interfacial area in packed columns. *Chem Eng J*. 1989;41:49–52.
63. Roesler J, Raynal L. Determination of liquid mass transfer characteristics in a high specific geometric area structured packing via chemical methods. Presented at *International Symposium on Chemical Reaction Engineering 19, Potsdam/Berlin*, 2006.
64. Danckwerts PV, Sharma MM. The absorption of carbon dioxide into solutions of alkalis and amines (with some notes on hydrogen sulphide and carbonyl sulphide). *Chem Eng Lond*. 1966;44:CE244–CE280.
65. Weisman J, Bonilla CF. Liquid-gas interfacial area in packed columns. *Ind Eng Chem*. 1950;42(6):1099–1105.
66. Shulman HL, Ullrich CF, Proulx AZ, Zimmerman JO. Performance of packed columns. II. Wetted and effective-interfacial areas, gas - and liquid - phase mass transfer rates. *AIChE J*. 1955;1(2):253–258.
67. Bravo JL, Fair JR. Generalized correlation for mass transfer in packed distillation columns. *Ind Eng Chem Process Des Dev*. 1982; 21:162–170.
68. Nakov S. Study of the influence of liquid phase viscosity on the effective surface area of arranged packings with vertical walls at low liquid superficial velocity. *Chem Eng Technol*. 2000;23(7):615–618.
69. Rejl FJ, Valenz L, Linek V. “Profile method” for the measurement of  $k_{L,a}$  and  $k_{V,a}$  in distillation column. Validation of rate- based distillation models using concentration profiles measured along the column. *Ind Eng Chem Res*. 2010;49:4383.
70. Gamson BW, Thodos G, Hougen OA. Heat, mass, and momentum transfer in the flow of gases through granular solids. *Trans Am Inst Chem Eng*. 1943;39:1–35.
71. Yoshida F, Koyanagi T. Mass transfer and effective interfacial areas in packed columns. *AIChE J*. 1962;8(3):309–316.
72. Taecker RG, Hougen OA. Heat, mass transfer of gas film in flow of gases through commercial tower packings. *Chem Eng Prog*. 1949; 45(3):188–193.
73. Yoshida F, Koyanagi T. Liquid phase mass transfer rates and effective interfacial area in packed absorption columns. *Ind Eng Chem*. 1958;50(3):365–374.
74. Hikita H, Kataoka T, Nakanishi K. Effective interfacial area for liquid phase mass transfer in packed columns. *Kagaku Kogaku*. 1960; 24(1):2–8.
75. Hikita H, Ono Y. Mass transfer into a liquid film flowing over a packing piece. *Kagaku Kogaku*. 1959;23(12):808–813.
76. Suess P, Spiegel L. Hold-up of Mellapak structured packings. *Chem Eng Process*. 1992;31:119–124.
77. Green CW, Farone J, Briley JK, Eldridge RB, Ketcham RA, Nightingale B. Novel application of X-ray computed tomography: determination of gas/liquid contact area and liquid holdup in structured packing. *Ind Eng Chem Res*. 2007;46:5734–5753.
78. Aferka S, Marchot P, Crine M, Toye D. Interfacial area measurement in a catalytic distillation packing using high energy X-ray CT. *Chem Eng Sci*. 2010;65(1):511–516.
79. Mayo F, Hunter TO, Sash AW. *J Soc Chem Ind*. 1935;54:375.
80. Fujita S, Sakuma S. Wetted area of Raschig rings in packed columns. *Kagaku Kogaku*. 1954;18(2):64–67.
81. Hikita H, Kataoka T. Wetted area in a packed column. *Kagaku Kogaku*. 1956;20(10):528–533.
82. Onda K, Takeuchi H, Koyama Y. Effect of packing materials on the wetted surface area. *Kagaku Kogaku*. 1967;31(2):126–134.
83. Choi U, Kim JS. The determination of wetted area of packing materials. *Korean Chem Eng Res*. 1970;8(2):61–67.
84. Shulman HL, DeGouff JJ. Mass transfer coefficients and Interfacial areas for 1-inch Raschig rings. *Ind Eng Chem*. 1952;44(8):1915–1922.
85. Fellingner L. *Adsorption of Ammonia by Water and Acid in Various Standard Packings* [Dissertation]. Cambridge, MS: Massachusetts Institute of Technology, 1941.
86. Hensel SL, Treybal RE. Air-water contact-adiabatic humidification of air with water in a packed tower. *Chem Eng Prog*. 1952;48(7): 362–370.
87. Lynch EJ, Wilke CR. Effect of fluid properties on mass transfer in the gas phase. *AIChE J*. 1955;1(1):9–19.
88. Sherwood TK, Holloway FAL. Performance of packed towers—experimental studies of absorption and desorption. *Trans Am Inst Chem Eng*. 1940;36:21–37.
89. Van Krevelen DW, Hoftijzer PJ, Van Hooren CJ. Studies of gas absorption: III. Gas phase resistance to gas absorption in scrubbers. *Recl Trav Chim Pays-Bas*. 1947;66:513–531.
90. McAdams WH, Pohlentz JB, St. John RC. Transfer of heat and mass between air and water in a packed tower. *Chem Eng Prog*. 1949; 45(4):243–252.
91. Surosky AE, Dodge BF. Effect of diffusivity on gas-film absorption coefficients in packed towers. *Ind Eng Chem*. 1950;42(6):1112–1119.
92. Yoshida F, Tanaka T. Air-water contact operations in a packed column. *Ind Eng Chem*. 1951;43(6):1467–1473.
93. Yoshida F. Gas-film mass transfer in a packed column. *Chem Eng Prog Symp Ser*. 1955;51(16):59–67.
94. Shulman HL, Delaney LJ. Performance of packed columns: V. Effect of solute concentration on gas-phase mass transfer rates. *AIChE J*. 1959;5(3):290–294.
95. Shulman HL, Robinson RG. Performance of packed columns: VI. Mass transfer rates for dehumidification at high solute concentrations. *AIChE J*. 1960;6(3):469–472.
96. Onda K, Takeuchi H, Okumoto Y. Mass transfer coefficients between gas and liquid phases in packed columns. *J Chem Eng Jpn*. 1968;1(1):56–62.
97. Murrieta CR, Seibert AF, Fair JR, Rocha-U JA. Liquid-side mass-transfer resistance of structured packings. *Ind Eng Chem Res*. 2004; 43:7113–7120.
98. Sherwood TK, Holloway FAL. Performance of packed towers-liquid film data for several packings. *Trans Am Inst Chem Eng*. 1940;36:39–69.
99. Whitney RP, Vivian JE. Absorption of sulfur dioxide in water. *Chem Eng Prog*. 1949;45(5):323–337.
100. Sherwood TK. *Absorption and Extraction*. New York: McGraw-Hill, 1937.
101. Kowalke OL, Hougen OA, Watson KM. Transfer coefficients of ammonia in absorption towers. *Bull Univ Wis Eng Exp Stn*. 1925;68: 1–86.

102. Othmer DF, Scheibel EG. Acetone absorption by water in a semi-commercial packed tower. *Trans Am Inst Chem Eng.* 1941;37:211–234.
103. White RE, Othmer DF. Gas absorption in Stedman packed column. *Trans Am Inst Chem Eng.* 1942;38:1067–1087.
104. Scheibel EG, Othmer DF. Gas absorption as a function of diffusivities and flow rates. *Trans Am Inst Chem Eng.* 1944;40:611–653.
105. Dwyer OE, Dodge BF. Rate of absorption of ammonia by water in a packed tower. *Ind Eng Chem.* 1941;33(4):485–492.
106. Gross WF, Simmons CW. Countercurrent absorption in non-aqueous systems. *Trans Am Inst Chem Eng.* 1944;40:121–141.
107. Molstad MC, McKinney JF, Abbey RG. Performance of drip-point grid tower packings III. Gas-film mass transfer coefficients; additional liquid-film mass transfer coefficients. *Trans Am Inst Chem Eng.* 1943;39:605–660.
108. Landau R, Birchenall CE, Joris GG, Elgin JC. Absorption in a high molecular weight non-aqueous system - uranium hexafluoride in heavy oil. *Chem Eng Prog.* 1948;44(4):315–326.
109. Hutchings LE, Stutzman LF, Koch HA. Gas absorption-mass transfer coefficients as function of liquid, gas rates, tower packing characteristics. *Chem Eng Prog.* 1949;45(4):253–268.
110. Molstad MC, Parsly LF. Performance of drip-point grid tower packings V. Absorption of ethanol vapor. *Chem Eng Prog.* 1950;46(1):20–28.
111. Houston RW, Walker CA. Absorption in packed towers. Effect of molecular diffusing on gas film coefficient. *Ind Eng Chem.* 1950;42(6):1105–1112.
112. Zabban W, Dodge BF. Effect of total pressure on the gas-film absorption coefficient in a packed tower. *Chem Eng Prog Symp Ser.* 1954;10:61–72.
113. Onda K, Sada E, Saito M. Gas-side mass transfer coefficients in packed tower. *Kagaku Kogaku.* 1961;25(11):820–829.
114. Billet R, Maćkowiak J. Development and process characteristics of Impulse Packing for gas-liquid systems. *Fette Seifen Anstrichm.* 1983;85(10):383–391.
115. Maćkowiak J. Untersuchungen des gas- und flüssigkeitsseitigen Stoffüberganges in Kolonnen mit strukturierten Packungen. *Chem Ing Tech.* 1999;1–2(71):100–104.
116. San-Valero P, Penya-Roja JM, Álvarez-Hornos FJ, Gabaldón C. Modelling mass transfer properties in a biotrickling filter for the removal of isopropanol. *Chem. Eng. Sci.* 2014;108:47–56.
117. Johnstone HF, Singh AD. Recovery of sulfur dioxide from waste gases-design of scrubbers for large quantities of gases. *Ind Eng Chem.* 1937;29(3):286–297.
118. Van Krevelen DW, Hoftijzer PJ, Van Hooren CJ. Studies of gas absorption. IV. Simultaneous gas absorption and chemical reaction. *Recl Trav Chim Pays-Bas.* 1948;67:133–152.
119. Nakov S, Kolev N. Performance characteristics of a packing with boundary layer turbulizers. IV. Gas-film controlled mass transfer. *Chem Eng Process.* 1994;33:443–448.
120. Moucha T, Linek V, Prokopová E. Effect of packing geometrical details - influence of free tips on volumetric mass transfer. *Chem Eng Res Des.* 2005;83(1):88–92.
121. Kim S, Deshusses MA. Determination of mass transfer coefficients for packing materials used in biofilters and biotrickling filters for air pollution control. 1. Experimental results. *Chem Eng Sci.* 2008;63:841–855.
122. Payne JW, Dodge BF. Rate of absorption of carbon dioxide in water and in alkaline media. *Ind Eng Chem.* 1932;24(6):630–637.
123. Allen HV. Absorption of Carbon Dioxide in Aqueous Solutions. M. S. Thesis in Chemical Engineering, Massachusetts Institute of Technology, Cambridge, MA, 1938.
124. Van Krevelen DW, Hoftijzer PJ. Studies of gas absorption. I. Liquid film resistance to gas absorption in scrubbers. *Recl Trav Chim Pays-Bas.* 1947;66:49–65.
125. Koch HA, Stutzman LF, Blum HA, Hutchings LE. Gas absorption-liquid transfer coefficients for the carbon dioxide-air-water system. *Chem Eng Prog.* 1949;45(11):677–682.
126. Hikita H, Sugata M, Kamo K. Liquid film coefficients of commercial packings: gas absorption in a packed tower. *Kagaku Kogaku.* 1954;18(10):454–456.
127. Ueyama K, Hikita H, Nishigami K, Funahashi S. Liquid-film coefficient for small glass rings: gas absorption in a packed column. *Kagaku Kogaku.* 1954;18(2):68–72.
128. Fujita S, Hayakawa T. Liquid-film mass transfer coefficients in packed towers and rod-like irrigation towers. *Kagaku Kogaku.* 1956;20(3):113–117.
129. Onda K, Sada E, Otubo F. Liquid-side mass-transfer coefficient for a tower packed with Raschig rings. *Kagaku Kogaku.* 1958;22(4):194–199.
130. Hikita H, Kataoka T, Kondo H. Effect of packed height on liquid phase HTU for packed columns. *Kagaku Kogaku.* 1959;23(8):520–524.
131. Onda K, Sada E, Murase Y. Liquid-side mass transfer coefficients in packed towers. *AIChE J.* 1959;5(2):235–239.
132. Onda K, Sada E. Absorption of carbon-dioxide by various solvents in packed towers. *Kagaku Kogaku.* 1959;23:220–225.
133. Onda K, Sada E, Kido C, Tanaka A. Liquid-side and gas-side mass transfer coefficients in towers packed with spheres. *Kagaku Kogaku.* 1963;27(1):140–146.
134. De Waal KJA, Beek WJ. A comparison between chemical absorption with rapid first-order reactions and physical absorption in one packed column. *Chem Eng Sci.* 1967;22:585–593.
135. Merchuk JC, Nakanishi K, Yoshida F. Gas absorption with second-order chemical reaction in a packed column. *J Chem Eng Jpn.* 1970;3(1):62–67.
136. Maćkowiak J. Dissertation. TU Wrocław, Wrocław, Poland, 1975.
137. Mangers RJ, Ponter AB. Effect of viscosity on liquid film resistance to mass transfer in a packed column. *Ind Eng Chem Process Des Dev.* 1980;19:530–537.
138. Mangers RJ, Ponter AB. Liquid phase resistance to mass transfer in a laboratory absorption column packed with glass and polytetrafluoroethylene rings part I. The effects of flowrate sequence, repacking, packing. *Chem Eng J.* 1980;19:139–146.
139. Billet R, Maćkowiak J. Application of modern packings in thermal separation processes. *Chem Eng Technol.* 1988;11:213–227.
140. Molstad MC, Abbey RG, Thompson AR, McKinney JF. Performance of drip-point grid tower packings II. Liquid-film mass transfer data. *Trans Am Inst Chem Eng.* 1942;38:410–434.
141. Jones CH. B. *Chem. Eng. Thesis.* New York: Cooper Union, 1946.
142. Vivian JE, Whitney RP. Absorption of chlorine into water. *Chem Eng Prog.* 1947;12:691–702.
143. Deed DW, Schutz PW, Drew TB. Comparison of rectification and desorption in packed columns. *Ind. Eng. Chem.* 1947;39(6):766–774.
144. Vivian JE, King CJ. The mechanism of liquid-phase resistance to gas absorption in a packed column. *AIChE J.* 1964;10(2):221–227.
145. Henriques de Brito M, von Stockar U, Bomio P. Predicting the liquid-phase mass transfer coefficients- $k_L$ -for the Sulzer structured packing Mellapak. *Inst Chem Eng Symp Ser.* 1992;128:B137.
146. Kolev N, Nakov S. Performance characteristics of a packing with boundary layer turbulizers. III. Liquid film controlled mass transfer. *Chem Eng Process.* 1994;33:437–442.
147. Brunazzi E, Paglianti A. Liquid-film mass-transfer coefficient in a column equipped with structured packings. *Ind Eng Chem Res.* 1997;36:3792–3799.
148. Roesler J, Royon-Lebeaud A, Alix P. Liquid side mass transfer coefficient measurements in tall structured packing beds by reactive absorption with dilute MDEA solutions. *Paper Presented at 2016 AIChE Annual Meeting, San Francisco, CA, USA, November 13-18, 2016, Paper n°467941.*
149. Schug S, Arlt W. In-situ-Stoffübergangsmessungen mit Computertomographie: Auswahl des Testsystems. *Chem Ing Tech.* 2015;87(5):656–659.
150. Billet R. Contribution to packed columns scale-up in separation processes. *J Chem Ind Eng.* 1992;7(2):235–252.
151. Fair JR. Sorption processes for gas separation. *Chem Eng.* 1969;7:90.
152. Furnas CC, Bellinger F. Operating characteristics of packed column I. A new method of correlating gas absorption data. *Trans Am Inst Chem Eng.* 1938;34:251–286.
153. Tsai RE. Mass Transfer Area of Structured Packing. Ph.D. Dissertation, The University of Texas at Austin, Austin, TX, 2010.
154. Yeh NK. Liquid Phase Mass Transfer in Spray Contactors. Ph.D. Dissertation, University of Texas at Austin, Austin, TX, 2002.
155. Alix P, Raynal L. Characterisation of a high capacity structured packing for CO<sub>2</sub> capture. *Paper presented at WCCE8 Congress, July 2009; Montreal.*
156. Fujita S, Kurihara H, Wakita E. *Paper Presented at the Meeting of Soc. Chem. Engrs. (Japan), 1954, Tokyo.*
157. Olujic Z. Types of distillation column internals. In: Górak A, Olujic Z, editors. *Distillation: Equipment and Processes.* Amsterdam, The Netherlands: Academic Press, 2014:1–34.
158. Olujic Z. Effect of column diameter on pressure drop of a corrugated sheet structured packing. *Chem Eng Res Des.* 1999;77:505–510.

159. Górák A, Olujić Ž. *Distillation: Equipment and Processes*. Amsterdam: Academic Press, 2014.
160. Wagner I, Stichlmair J, Fair JR. Mass transfer in beds of modern, high-efficiency random packings. *Ind Eng Chem Res.* 1997;36(1):227–237.
161. Piché S, Grandjean BPA, Iliuta I, Larachi F. Interfacial mass transfer in randomly packed towers: a confident correlation for environmental applications. *Environ Sci Technol.* 2001;35:4817–4822.
162. Piché S, Grandjean BPA, Larachi F. Reconciliation procedure for gas-liquid interfacial area and mass-transfer coefficient in randomly packed towers. *Ind Eng Chem Res.* 2002;41:4911–4920.
163. Cornell DW, Knapp WG, Fair JR. Mass transfer efficiency - packed columns - part I. *Chem Eng Prog.* 1960; 56(7): 68–74.
164. Nawrocki PA, Chuang KT. Carbon dioxide absorption into a stable liquid rivulet. *Can J Chem Eng.* 1996;74:24.
165. Pelkonen S, Górák A, Ohligschläger A, Kaesemann R. Experimental study on multicomponent distillation in packed columns. *Chem Eng Process.* 2001;40:235–243.
166. Brettschneider O, Thiele R, Faber R, Thielert H, Wozny G. Experimental investigation and simulation of the chemical absorption in a packed column for the system NH<sub>3</sub>-CO<sub>2</sub>-H<sub>2</sub>S- NaOH-H<sub>2</sub>O. *Sep Purif Technol.* 2004;9:139–159.
167. Schultes M, Röhm HJ. *Forschungsaufgabe Stofftrennkolonnen - Alter Hut oder Dauerbrenner*. Würzburg: GVC-Fluid-Verfahrenstechnik, 2006.
168. Schultes M. Research on mass transfer columns: passé? *Chem Eng Technol.* 2013;36(9):1539–1549.
169. Billet R, Schultes M. Predicting mass transfer in packed columns. *Chem. Eng. Technol.* 1993;16(1):1–9.
170. Wolf V, Lehner M, Hoffmann K. Influences of the experimental setup configuration on mass transfer measurements in absorption systems. *Chem Eng Res Des.* 2015;99:228–235.
171. Kunze AK, Lutze P, Schoenmakers H, Müller S, Kopatschek M, Maćkowiak J, Maćkowiak J, Górák A, Grünewald M. Die Notwendigkeit einer Standardisierung von Stofftransportmessungen in der Ab- und Desorption. *Chem Ing Tech.* 2012;84(11):1931–1938.
172. Kunze AK, Górák A. *Project Report and Software "Standardisation of Mass Transfer Measurements of Absorption and Desorption."* Dortmund: Laboratory of Fluid Separations, TU Dortmund University. Available at <http://www.fvt.bci.tu-dortmund.de/cms/en/research/projects/completedprojects/Abso-Global-Standard/index.html> Updated: 04.01.2015, Accessed January 18, 2016.